

CMA-ES with Margin for Single-and Multi-Objective Mixed-Integer Black-Box Optimization

RYOKI HAMANO, Yokohama National University, Japan

SHOTA SAITO, Yokohama National University & SkillUp AI Co., Ltd., Japan

MASAHIRO NOMURA, CyberAgent, Japan

SHINICHI SHIRAKAWA, Yokohama National University, Japan

This study targets the mixed-integer black-box optimization (MI-BBO) problem where continuous and integer variables should be optimized simultaneously. The CMA-ES, our focus in this study, is a population-based stochastic search method that samples solution candidates from a multivariate Gaussian distribution (MGD), which shows excellent performance in continuous BBO. The parameters of MGD, mean and (co)variance, are updated based on the evaluation value of candidate solutions in the CMA-ES. If the CMA-ES is applied to the MI-BBO with straightforward discretization, however, the variance corresponding to the integer variables becomes much smaller than the granularity of the discretization before reaching the optimal solution, which leads to the stagnation of the optimization. In particular, when binary variables are included in the problem, this stagnation more likely occurs because the granularity of the discretization becomes wider, and the existing modification to the CMA-ES does not address this stagnation. To overcome these limitations, we propose a simple extension of the CMA-ES based on lower-bounding the marginal probabilities associated with the generation of integer variables in the MGD. The numerical experiments on the MI-BBO benchmark problems demonstrate the efficiency and robustness of the proposed method. Furthermore, in order to demonstrate the generality of the idea of the proposed method, in addition to the single-objective optimization case, we incorporate it into multi-objective CMA-ES and verify its performance on bi-objective mixed-integer benchmark problems.

CCS Concepts: • Mathematics of computing → Mixed discrete-continuous optimization.

Additional Key Words and Phrases: covariance matrix adaptation evolution strategy, mixed-integer black-box optimization

ACM Reference Format:

Ryoki Hamano, Shota Saito, Masahiro Nomura, and Shinichi Shirakawa. 2018. CMA-ES with Margin for Single-and Multi-Objective Mixed-Integer Black-Box Optimization. 1, 1 (December 2018), 25 pages. <https://doi.org/XXXXXX.XXXXXXX>

1 INTRODUCTION

The mixed-integer black-box optimization (MI-BBO) problem is the problem of simultaneously optimizing continuous and integer variables under the condition that the objective function is not differentiable and not available in the explicit functional form. The MI-BBO problems often appear in real-world applications such as, material design [Iyer et al. 2020; Zhang et al. 2020], topology optimization [Fujii et al. 2018; Yang and Kao 1998], placement optimization for CO₂ capture and storage [Miyagi et al. 2018], and hyper-parameter optimization of machine learning [Hazan et al. 2018; Hutter

Authors' addresses: Ryoki Hamano, Yokohama National University, Yokohama, Kanagawa, Japan, hamano-ryoki-pd@ynu.jp; Shota Saito, Yokohama National University & SkillUp AI Co., Ltd., Yokohama, Kanagawa, Japan, saito-shota-bt@ynu.jp; Masahiro Nomura, CyberAgent, Shibuya, Tokyo, Japan, nomura_masahiro@cyberagent.co.jp; Shinichi Shirakawa, Yokohama National University, Yokohama, Kanagawa, Japan, shirakawa-shinichi-bg@ynu.ac.jp.

Permission to make digital or hard copies of all or part of this work for personal or classroom use is granted without fee provided that copies are not made or distributed for profit or commercial advantage and that copies bear this notice and the full citation on the first page. Copyrights for components of this work owned by others than ACM must be honored. Abstracting with credit is permitted. To copy otherwise, or republish, to post on servers or to redistribute to lists, requires prior specific permission and/or a fee. Request permissions from permissions@acm.org.

© 2018 Association for Computing Machinery.

Manuscript submitted to ACM

et al. 2019]. Several algorithms have been designed for MI-BBO so far, e.g., the extended evolution strategies [Li et al. 2013] and surrogate model-based method [Blietk et al. 2021]. However, despite the high demand for an efficient MI-BBO method, the BBO methods for mixed-integer problems are not actively developed compared to those for continuous or discrete problems. One common way is applying a continuous BBO method to an MI-BBO problem by discretizing the continuous variables when evaluating a candidate solution rather than using a specialized method for MI-BBO.

The *covariance matrix adaptation evolution strategy* (CMA-ES) [Hansen et al. 2003; Hansen and Ostermeier 1996] is a powerful method in continuous black-box optimization, aiming to minimize the objective function through population-based stochastic search. The CMA-ES samples several continuous vectors from a multivariate Gaussian distribution (MGD) and then evaluates the objective function values of the vectors. Subsequently, the CMA-ES facilitates optimization by updating the mean vector, covariance matrix, and step-size (overall standard deviation) based on evaluation values. The CMA-ES exhibits two attractive properties for users. First, it has several invariance properties, such as the invariance of a strictly monotonic transformation of the objective function and an affine transformation (rotation and translation) of the search space. These invariances make it possible to generalize the powerful empirical performance of the CMA-ES of one particular problem to another. Second, the CMA-ES is a quasi-parameter-free algorithm, which allows use without tuning the hyperparameters, such as the learning rate for the mean vector or covariance matrix. In the CMA-ES, all hyperparameters are given default values based on theoretical work and careful experiments.

The most straightforward way to apply the CMA-ES to the MI-BBO is to discretize some elements of the sampled continuous vector, e.g., [Tamilselvi and Baskar 2014]. However, because of the plateau caused by the discretization, this simple method may not change the evaluation value by small variations in elements corresponding to the integer variables. Specifically, as pointed out in [Hansen 2011], this stagnation occurs when the sample standard deviation of the dimension corresponding to an integer variable becomes much smaller than the granularity of the discretization. In particular, the step-size tends to decrease with each iteration, which promotes trapping on the plateau of the integer variables. To address this plateau problem in the integer variable treatment, Hansen [2011] proposed the injection of mutations into a sample of elements corresponding to integer variables in the CMA-ES, and Miyagi et al. [2018] used this modification for the real-world MI-BBO problem. Although this mutation injection is effective on certain problem classes, Hansen [2011] mentioned that it is not suitable for binary variables or k -ary integers in $k < 10$.

This study aims to improve the integer variable treatment of the CMA-ES in the MI-BBO problem. First, we investigate why the CMA-ES search fails in MI-BBO problems involving binary variables. Following the result, we propose the adaptation of the sample discretization process according to the current MGD parameters. The proposed adaptive discretization process can be represented as an affine transformation for a sample. Therefore, owing to the affine invariance of CMA-ES, it is expected to maintain the good behavior of the original CMA-ES. Additionally, we extend the proposed method from binary variables to integer variables.

The proposed method, termed CMA-ES with Margin, has the advantage of high generality because it is based on a simple and principled idea, lower-bounding the marginal probabilities associated with the generation of integer variables in the MGD. To demonstrate the generality of the idea of the proposed method, in addition to the single-objective optimization case, we also develop an extension of the CMA-ES with Margin for multi-objective optimization. Specifically, we introduce the idea of CMA-ES with Margin into the MO-CMA-ES (multi-objective covariance matrix adaptation) [Igel et al. 2007; Voß et al. 2010]. This part is the extension from the previous work [Hamano et al. 2022]. We empirically evaluate the behavior of the method, MO-CMA-ES with Margin, through experiments on bi-objective mixed-integer benchmark problems.

Table 1. Default hyperparameters and initial values of the CMA-ES.

λ	$4 + \lfloor 3 \ln(N) \rfloor$
μ	$\lfloor \frac{\lambda}{2} \rfloor$
w'_i	$\ln\left(\frac{\lambda+1}{2}\right) - \ln i$
$w_i(i \leq \mu)$	$\frac{w'_i}{\sum_{j=1}^{\mu} w'_j}$
$w_i(i > \mu)$	$\frac{w'_i}{\sum_{j=\mu+1}^{\lambda} w'_j } \min\left(1 + \frac{c_1}{c_\mu}, 1 + \frac{2\mu_w}{\mu_w+2}, \frac{1-c_1-c_\mu}{Nc_\mu}\right)$
μ_w	$\frac{1}{\sum_{j=1}^{\mu} (w'_j)^2}$
μ_w^-	$\frac{\left(\sum_{j=\mu+1}^{\lambda} w'_j\right)^2}{\sum_{j=\mu+1}^{\lambda} (w'_j)^2}$
c_m	1
c_σ	$\frac{\mu_w+2}{N+\mu_w+5}$
c_c	$\frac{4+\mu_w/N}{N+4+2\mu_w/N}$
c_1	$\frac{2}{(N+1.3)^2+\mu_w}$
c_μ	$\min\left(1 - c_1, \frac{2(\mu_w-2+1/\mu_w)}{(N+2)^2+\mu_w}\right)$
d_σ	$1 + c_\sigma + 2 \max\left(0, \sqrt{\frac{\mu_w-1}{N+1}} - 1\right)$
$p_\sigma^{(0)}, p_c^{(0)}$	0
$\mathbf{m}^{(0)}, C^{(0)}, \sigma^{(0)}$	Depending on the problem

The rest of this paper is organized as follows. In Section 2, we describe the CMA-ES and the existing method of mixed-integer handling [Hansen 2011]. In Section 3, we conduct numerical experiments to clarify why the existing mixed-integer handling is difficult to optimize binary variables. In Section 4, we propose a simple extension of the CMA-ES for the MI-BBO. In Section 5, we apply the proposed method to the MI-BBO problems to validate its robustness and efficiency. Furthermore, to demonstrate the generality of the idea of the proposed method, in Section 6, we develop an extension of the CMA-ES with Margin for multi-objective optimization, and we empirically analyze its behavior on bi-objective benchmark problems in Section 7. Section 8 concludes with summary and future direction of this work.

2 CMA-ES AND MIXED INTEGER HANDLING

2.1 CMA-ES

Let us consider the black-box minimization problem in the continuous search space for an objective function $f : \mathbb{R}^N \rightarrow \mathbb{R}$. The CMA-ES samples an N -dimensional candidate solution $\mathbf{x} \in \mathbb{R}^N$ from an MGD $\mathcal{N}(\mathbf{m}, \sigma^2 C)$ parameterized by the mean vector $\mathbf{m} \in \mathbb{R}^N$, covariance matrix $C \in \mathbb{R}^{N \times N}$, and step-size $\sigma \in \mathbb{R}_{>0}$. The CMA-ES updates the distribution parameters based on the objective function value $f(\mathbf{x})$. There are several variations in the update methods of distribution parameters, although we consider the de facto standard CMA-ES [Hansen 2016], which combines the weighted recombination, cumulative step-size adaptation, rank-one covariance matrix update, and rank- μ update. We use the default parameters proposed in [Hansen 2016] and list them in Table 1. The CMA-ES repeats the following steps until a termination criterion is satisfied.

Sample and Evaluate Candidate Solutions. In the t -th iteration, the λ candidate solutions \mathbf{x}_i ($i = 1, 2, \dots, \lambda$) are sampled independently from the MGD $\mathcal{N}(\mathbf{m}^{(t)}, (\sigma^{(t)})^2 C^{(t)})$ as follows:

$$\mathbf{y}_i = (C^{(t)})^{\frac{1}{2}} \xi_i , \quad (1)$$

$$\mathbf{x}_i = \mathbf{m}^{(t)} + \sigma^{(t)} \mathbf{y}_i , \quad (2)$$

where $\xi_i \sim \mathcal{N}(\mathbf{0}, \mathbf{I})$ represents a random vector with zero mean and a covariance matrix of the identity matrix \mathbf{I} , and $(C^{(t)})^{\frac{1}{2}}$ is the square root of the covariance matrix $C^{(t)}$ that is the symmetric and positive definite matrix satisfying $C^{(t)} = (C^{(t)})^{\frac{1}{2}} (C^{(t)})^{\frac{1}{2}}$. The candidate solutions $\{\mathbf{x}_1, \mathbf{x}_2, \dots, \mathbf{x}_\lambda\}$ are evaluated by f and sorted by ranking. Let $\mathbf{x}_{i:\lambda}$ be the i -th best candidate solution; then, $f(\mathbf{x}_{1:\lambda}) \leq f(\mathbf{x}_{2:\lambda}) \leq \dots \leq f(\mathbf{x}_{\lambda:\lambda})$ and let $\mathbf{y}_{i:\lambda}$ be the random vector corresponding to $\mathbf{x}_{i:\lambda}$.

Update Mean Vector. The mean vector update uses the weighted sum of the best $\mu < \lambda$ candidate solutions and updates $\mathbf{m}^{(t)}$ as follows:

$$\mathbf{m}^{(t+1)} = \mathbf{m}^{(t)} + c_m \sum_{i=1}^{\mu} w_i (\mathbf{x}_{i:\lambda} - \mathbf{m}^{(t)}) , \quad (3)$$

where c_m is the learning rate for the mean vector, and the weight w_i satisfies $w_1 \geq w_2 \geq \dots \geq w_\mu > 0$ and $\sum_{i=1}^{\mu} w_i = 1$.

Compute Evolution Paths. For the step-size adaptation and the rank-one update of the covariance matrix, we use evolution paths that accumulate an exponentially fading pathway of the mean vector in the generation sequence. Let \mathbf{p}_σ and \mathbf{p}_c describe the evolution paths for the step-size adaptation and rank-one update, respectively; then, $\mathbf{p}_\sigma^{(t)}$ and $\mathbf{p}_c^{(t)}$ are updated as follows:

$$\mathbf{p}_\sigma^{(t+1)} = (1 - c_\sigma) \mathbf{p}_\sigma^{(t)} + \sqrt{c_\sigma(2 - c_\sigma)\mu_w} C^{(t)}^{-\frac{1}{2}} \sum_{i=1}^{\mu} w_i \mathbf{y}_{i:\lambda} , \quad (4)$$

$$\mathbf{p}_c^{(t+1)} = (1 - c_c) \mathbf{p}_c^{(t)} + h_\sigma \sqrt{c_c(2 - c_c)\mu_w} \sum_{i=1}^{\mu} w_i \mathbf{y}_{i:\lambda} , \quad (5)$$

where c_σ and c_c are cumulative rates, μ_w is effective sample-size, and

$$h_\sigma = \mathbb{1} \left\{ \|\mathbf{p}_\sigma^{(t+1)}\| < \sqrt{1 - (1 - c_\sigma)^2(t+1)} \left(1.4 + \frac{2}{N+1} \right) \mathbb{E}[\|\mathcal{N}(\mathbf{0}, \mathbf{I})\|] \right\}$$

is an indicator function used to suppress a rapid increase in \mathbf{p}_c , where $\mathbb{E}[\|\mathcal{N}(\mathbf{0}, \mathbf{I})\|] \approx \sqrt{N} \left(1 - \frac{1}{4N} + \frac{1}{21N^2} \right)$ is the expected Euclidean norm of the sample from a standard Gaussian distribution.

Update Step-size and Covariance Matrix. Using the evolution paths computed in the previous step, we update $C^{(t)}$ and $\sigma^{(t)}$ as follows:

$$C^{(t+1)} = \left(1 - c_1 - c_\mu \sum_{i=1}^{\lambda} w_i + (1 - h_\sigma) c_1 c_c (2 - c_c) \right) C^{(t)} + \underbrace{c_1 \mathbf{p}_c^{(t+1)} \mathbf{p}_c^{(t+1)\top}}_{\text{rank-one update}} + \underbrace{c_\mu \sum_{i=1}^{\lambda} w_i^\circ \mathbf{y}_{i:\lambda} \mathbf{y}_{i:\lambda}^\top}_{\text{rank-}\mu\text{ update}} , \quad (6)$$

$$\sigma^{(t+1)} = \sigma^{(t)} \exp \left(\frac{c_\sigma}{d_\sigma} \left(\frac{\|\mathbf{p}_\sigma^{(t+1)}\|}{\mathbb{E}[\|\mathcal{N}(\mathbf{0}, \mathbf{I})\|]} - 1 \right) \right) , \quad (7)$$

where $w_i^\circ := w_i \cdot \left(1 \text{ if } w_i \geq 0 \text{ else } N/\left\| (C^{(t)})^{-\frac{1}{2}} \mathbf{y}_{i:\lambda} \right\|^2\right)$, c_1 and c_μ are the learning rates for the rank-one and rank- μ updates, respectively. Additionally, d_σ is a damping parameter for the step-size adaptation.

2.2 CMA-ES with Mixed-Integer Handling

In [Hansen 2011], several steps of the CMA-ES are modified to handle the integer variables. To explain this modification, we apply notations $[\cdot]_j$ and $\langle \cdot \rangle_j$, where the former denotes the j -th element of an argument vector and the latter denotes the j -th diagonal element of an argument matrix. We denote the number of dimensions as $N = N_{\text{co}} + N_{\text{in}}$, where N_{co} and N_{in} are the numbers of the continuous and integer variables, respectively. More specifically, the 1st to N_{co} -th elements and $(N_{\text{co}} + 1)$ -th to N -th elements of the candidate solution are the elements corresponding to the continuous and integer variables, respectively.

Inject Integer Mutation. For the element corresponding to the integer variable, stagnation occurs when the sample standard deviation becomes much smaller than the granularity of the discretization. The main idea to solve this stagnation in [Hansen 2011] is to inject the *integer mutation vector* $\mathbf{r}_i^{\text{int}} \in \mathbb{N}^N$ into the candidate solution, which is given by

$$\mathbf{x}_i = \mathbf{m}^{(t)} + \sigma^{(t)} \mathbf{y}_i + \mathbf{S}^{\text{int}} \mathbf{r}_i^{\text{int}}, \quad (8)$$

where \mathbf{S}^{int} is the diagonal matrix whose diagonal elements indicate the variable granularities, which is $\langle \mathbf{S}^{\text{int}} \rangle_j = 1$ if $N_{\text{co}} + 1 \leq j \leq N$; otherwise $\langle \mathbf{S}^{\text{int}} \rangle_j = 0$ in usual case. The integer mutation vector $\mathbf{r}_i^{\text{int}}$ is sampled as follows:

Step 1. Set up a randomly ordered set of elements indices $J^{(t)}$ satisfying $2\sigma^{(t)} \langle C^{(t)} \rangle_j^{\frac{1}{2}} < \langle \mathbf{S}^{\text{int}} \rangle_j$.
Step 2. Determine the number of candidate solutions into which the integer mutation is injected as follows:

$$\lambda_{\text{int}}^{(t)} = \begin{cases} 0 & (|J^{(t)}| = 0) \\ \min(\lambda/10 + |J^{(t)}| + 1, \lfloor \lambda/2 \rfloor - 1) & (0 < |J^{(t)}| < N) \\ \lfloor \lambda/2 \rfloor & (|J^{(t)}| = N) \end{cases}.$$

Step 3. $[R'_i]_j = 1$ if the element indicate j is equal to $\text{mod}(i - 1, |J^{(t)}|)$ -th element of $J^{(t)}$, otherwise $[R'_i]_j = 0$.
Step 4. $[R''_i]_j$ is sampled from a geometric distribution with the probability parameter $p = 0.7^{\frac{1}{|J^{(t)}|}}$ if $j \in J^{(t)}$, otherwise $[R''_i]_j = 0$.
Step 5. $\mathbf{r}_i^{\text{int}} = \pm(R'_i + R''_i)$ with the sign-switching probability 1/2 if $i \leq \lambda_{\text{int}}^{(t)}$, otherwise $\mathbf{r}_i^{\text{int}} = 0$.
Step 6. If $\lambda_{\text{int}}^{(t)} > 0$, $[\mathbf{r}_\lambda^{\text{int}}]_j = \pm \left(\left\lfloor \frac{[\mathbf{x}_{1:\lambda}^{(t-1)}]_j}{\langle \mathbf{S}^{\text{int}} \rangle_j} \right\rfloor - \left\lfloor \frac{[\mathbf{m}^{(t)}]_j}{\langle \mathbf{S}^{\text{int}} \rangle_j} \right\rfloor \right)$ with the sign-switching probability 1/2 if $\langle \mathbf{S}^{\text{int}} \rangle_j > 0$, otherwise $[\mathbf{r}_\lambda^{\text{int}}]_j = 0$. This is a modified version of [Hansen 2011] and introduced in [Miyagi et al. 2018].

Modify Step-size Adaptation. If the standard deviation of the elements corresponding to the integer variables is much smaller than the granularity of the discretization, then the step-size adaptation rapidly decreases the step-size. To address this problem, [Hansen 2011] proposed a modification of the step-size adaptation to remove the elements corresponding to integer variables with considerably smaller standard deviations from the evolution path $\mathbf{p}_\sigma^{(t+1)}$ when updating the step-size as follows:

$$\sigma^{(t+1)} = \sigma^{(t)} \exp \left(\frac{c_\sigma}{d_\sigma} \left(\frac{\|I_\sigma^{(t+1)} \mathbf{p}_\sigma^{(t+1)}\|}{\mathbb{E}[\|\mathcal{N}(\mathbf{0}, I_\sigma^{(t+1)})\|]} - 1 \right) \right), \quad (9)$$

where $I_\sigma^{(t+1)}$ is the diagonal masking matrix, and $\langle I_\sigma^{(t+1)} \rangle_j = 0$ if $5\sigma \langle C^{(t)} \rangle_j^{\frac{1}{2}} / \sqrt{c_\sigma} < \langle S^{\text{int}} \rangle_j$; otherwise, $\langle I_\sigma^{(t+1)} \rangle_j = 1$. The expected value $\|\mathcal{N}(0, I_\sigma^{(t+1)})\|$ is approximated by $\sqrt{M} \left(1 - \frac{1}{4M} + \frac{1}{21M^2}\right)$, where M is the number of non-zero diagonal elements for $I_\sigma^{(t+1)}$.

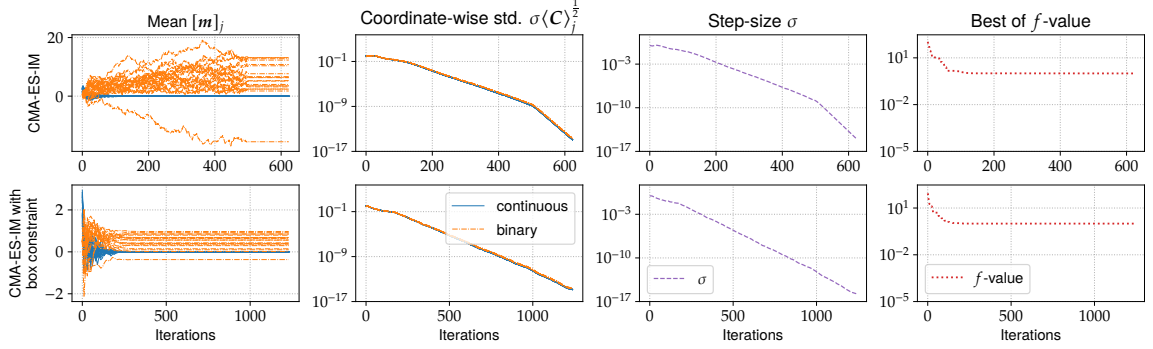


Fig. 1. Transition of each element of the mean vector and the diagonal elements of the covariance matrix on CMA-ES-IM [Hansen 2011] with and without the box constraint for a typical single failed trial on 40-dimensional SPHEREONEMAX.

3 PRELIMINARY EXPERIMENT: WHY IS IT DIFFICULT TO OPTIMIZE BINARY VARIABLES?

It is known that the integer variable handling of CMA-ES [Hansen 2011] does not work well for binary variables. However, the reasons for this have not been well explored. We then empirically check why this integer handling fails to optimize binary variables.

We consider the function $\text{ENCODING}_f(\mathbf{x}_i)$ to binarize the elements of the candidate solution corresponding to the binary variables, and the dimension $N = N_{\text{co}} + N_{\text{bi}}$, where N_{bi} is the number of binary variables. We define $\text{ENCODING}_f(\mathbf{x}_i) : \mathbb{R}^{N_{\text{co}}} \times \mathbb{R}^{N_{\text{bi}}} \mapsto \mathbb{R}^{N_{\text{co}}} \times \{0, 1\}^{N_{\text{bi}}}$ as

$$\text{ENCODING}_f(\mathbf{x}_i) = \begin{cases} [\mathbf{x}_i]_j & (1 \leq j \leq N_{\text{co}}) \\ \mathbb{1}\{[\mathbf{x}_i]_j > 0\} & (N_{\text{co}} + 1 \leq j \leq N) \end{cases} . \quad (10)$$

The partially discretized candidate solution obtained by (10) is denoted by $\bar{\mathbf{x}}_i = \text{ENCODING}_f(\mathbf{x}_i)$.

Compared to the integer variables, binary variables have a much wider interval, where the same binary variables can be taken after binarization. Therefore, if the variance decreases while the mean vector is so far from the threshold zero at which the binary variable changes, the optimization of the binary variable fails.

Settings. We use the SPHEREONEMAX function as the objective function, which is a combination of the SPHERE function and the ONEMAX function for the continuous and binary variables, respectively. The SPHEREONEMAX function is defined as

$$\text{SPHEREONEMAX}(\bar{\mathbf{x}}_i) = \sum_{j=1}^{N_{\text{co}}} [\bar{\mathbf{x}}_i]_j^2 + N_{\text{bi}} - \sum_{k=N_{\text{co}}+1}^N [\bar{\mathbf{x}}_i]_k , \quad (11)$$

where the optimal solution is 0 for continuous variables and 1 for binary variables, respectively, and $\text{SPHEREONEMAX}(\bar{\mathbf{x}}^*) = 0$. We check the behavior using the CMA-ES with integer variable handling introduced in Section 2.2. Additionally, we use this CMA-ES variant with a box constraint $[\mathbf{x}_i]_j \in [-1, 1]$ corresponding to the binary variables. When the box

constraint is used, the penalty $\|\mathbf{x}_i^{\text{feas}} - \mathbf{x}_i\|_2^2/N$ is added to the evaluation value, where $\mathbf{x}_i^{\text{feas}}$ is the nearest-neighbor feasible solution to \mathbf{x}_i . The number of dimensions N is set to 40, and $N_{\text{co}} = N_{\text{bi}} = N/2 = 20$.

The initial mean vector $\mathbf{m}^{(0)}$ is set to uniform random values in the range [1, 3] for continuous variables and 0 for the binary variables, respectively. The covariance matrix and step-size are initialized with $C^{(0)} = \mathbf{I}$ and $\sigma^{(0)} = 1$, respectively. The optimization is successful when the best-evaluated value is less than 10^{-10} , and the optimization is stopped when the minimum eigenvalue of $\sigma^2 C$ is less than 10^{-30} .

Result and Discussion. For the coordinate-wise mean $[\mathbf{m}]_j$, the coordinate-wise standard deviation $\sigma \langle C \rangle_j^{\frac{1}{2}}$, step-size σ , and best-evaluated value, the upper and lower sides of the Figure 1 show the transitions of a single typical run of the optimization failure for the CMA-ES with the integer mutation and modification of the step-size adaptation (denoted by CMA-ES-IM) and the CMA-ES-IM with the box constraint. The CMA-ES-IM decreases the coordinate-wise standard deviations for binary variables with the step-size. In contrast, coordinate-wise mean is far from the threshold value of zero. In this case, the integer mutation provided in Step 1 to Step 5 in Section 2.2 is not effective to improve the evaluation value because in the dimension corresponding to the binary variable, $S^{\text{int}} \mathbf{r}_i^{\text{int}}$ ($i = 1, \dots, \lambda_{\text{int}}^{(t)}$) are smaller than the distances between $\mathbf{m}^{(t)} + \sigma^{(t)} \mathbf{y}_i$ and the threshold value of zero. Moreover, when $S^{\text{int}} \mathbf{r}_{\lambda}^{\text{int}}$ calculated in Step 6 also becomes small, the mutation no longer affects the candidate solutions at all (after 500 iterations in Figure 1).

On the other hand, CMA-ES-IM with box constraint can prevent the coordinate-wise mean from being far from zero and avoid fixation of candidate solutions by the mutation. However, even if the mutation works, a high penalty value of box constraint results in a poor evaluation value. In this case, the mutated samples cannot be reflected in the mean update, which uses only the superior μ samples. Then, the stagnation problem in the negative domain still remains.

These results suggest that we need a new way to handle integer variables that takes binary variables into account instead of the integer mutation. In Section 4, we propose an integer handling method that preserves the generation probability of a different integer variable by introducing a correction that brings the coordinate-wise mean closer to a threshold value as the coordinate-wise standard deviation decreases.

4 PROPOSED METHOD

In this section, we propose a simple modification of the CMA-ES in the MI-BBO. The basic idea is to introduce a lower bound on the marginal probability referred to as the *margin*, so that the sample is not fixed to a single integer variable. The margin is a common technique in the estimation of distribution algorithms (EDAs) for binary domains to address the problem of bits being fixed to 0 or 1. In fact, the population-based incremental learning (PBIL) [Baluja 1994], a binary variable optimization method based on Bernoulli distribution, restricts the updated marginals to the range $[1/N, 1 - 1/N]$. This prevents the optimization from stagnating with the distribution converging to an undesirable direction before finding the optimum.

To introduce this margin correction to the CMA-ES, we define a diagonal matrix \mathbf{A} whose initial value is given by the identity matrix and redefine the MGD that generates the samples as $\mathcal{N}(\mathbf{m}, \sigma^2 \mathbf{A} \mathbf{C} \mathbf{A}^T)$. The margin correction is achieved by correcting \mathbf{A} and \mathbf{m} so that the probability of the integer variables being generated outside the dominant values is maintained above a certain value α . Because the sample generated from $\mathcal{N}(\mathbf{m}, \sigma^2 \mathbf{A} \mathbf{C} \mathbf{A}^T)$ is equivalent to applying the affine transformation of \mathbf{A} to the sample generated from $\mathcal{N}(\mathbf{m}, \sigma^2 \mathbf{C})$, we can separate the adaptation of the covariance and the update of \mathbf{A} . Consequently, the proposed modification can be represented as the affine transformation of the samples used to evaluate the objective function, without making any changes to the updates in CMA-ES. It should be

noted that although the mean vector can also be corrected by the affine transformation, we directly correct it to avoid the divergence of \mathbf{m} .

In this section, we first redefine ENCODING_f to facilitate the introduction of the margin. Next, we show the process of the CMA-ES with the proposed modification. Finally, we explain the margin correction, namely, the updates of \mathbf{A} and \mathbf{m} , separately for the cases of binary and integer variables.

4.1 Definition of ENCODING_f and Threshold ℓ

Let $z_{j,k}$ be the k -th smallest value among the discrete values in the j -th dimension, where $N_{\text{co}} + 1 \leq j \leq N$ and $1 \leq k \leq K_j$. It should be noted that K_j is the number of candidate integers for the j -th variable z_j . Under this definition, the binary variable can also be represented as, e.g. $z_{j,1} = 0, z_{j,2} = 1$. Moreover, we introduce a threshold ℓ for encoding continuous variables into discrete variables. Let $\ell_{j,k|k+1}$ be the threshold of two discrete variables $z_{j,k}$ and $z_{j,k+1}$; it is given by the midpoint of $z_{j,k}$ and $z_{j,k+1}$, namely, $\ell_{j,k|k+1} := (z_{j,k} + z_{j,k+1})/2$. We then redefine ENCODING_f when $N_{\text{co}} + 1 \leq j \leq N$ as follows:

$$\text{ENCODING}_f([\mathbf{x}_i]_j) = \begin{cases} z_{j,1} & \text{if } [\mathbf{x}_i]_j \leq \ell_{j,1|2} \\ z_{j,k} & \text{if } \ell_{j,k-1|k} < [\mathbf{x}_i]_j \leq \ell_{j,k|k+1} \\ z_{j,K_j} & \text{if } \ell_{j,K_j-1|K_j} < [\mathbf{x}_i]_j \end{cases}$$

Moreover, if $1 \leq j \leq N_{\text{co}}$, $[\mathbf{x}_i]_j$ is isometrically mapped as $\text{ENCODING}_f([\mathbf{x}_i]_j) = [\mathbf{x}_i]_j$. Then, the discretized candidate solution is denoted by $\bar{\mathbf{x}}_i = \text{ENCODING}_f(\mathbf{x}_i)$. The set of discrete variables z_j is not limited to consecutive integers such as $\{0, 1, 2\}$, but can also handle general discrete variables such as $\{1, 2, 4\}$ and $\{0.01, 0.1, 1\}$.

4.2 CMA-ES with the Proposed Modification

Given $\mathbf{A}^{(0)}$ as an identity matrix \mathbf{I} , the update of the proposed method, termed *CMA-ES with margin*, at the iteration t is given in the following steps.

- Step 1. The λ candidate solutions \mathbf{x}_i ($i = 1, 2, \dots, \lambda$) are sampled from $\mathcal{N}(\mathbf{m}^{(t)}, (\sigma^{(t)})^2 \mathbf{C}^{(t)})$ as $\mathbf{x}_i = \mathbf{m}^{(t)} + \sigma^{(t)} \mathbf{y}_i$, where $\mathbf{y}_i \sim \mathcal{N}(\mathbf{0}, \mathbf{C}^{(t)})$ for $i = 1, 2, \dots, \lambda$.
- Step 2. The affine transformed solutions \mathbf{v}_i ($i = 1, 2, \dots, \lambda$) are calculated as $\mathbf{v}_i = \mathbf{m}^{(t)} + \sigma^{(t)} \mathbf{A}^{(t)} \mathbf{y}_i$ for $i = 1, 2, \dots, \lambda$.
- Step 3. The discretized \mathbf{v}_i , i.e., $\bar{\mathbf{v}}_i$ ($i = 1, 2, \dots, \lambda$) are evaluated by f and sort $\{\mathbf{x}_{1:\lambda}, \mathbf{x}_{2:\lambda}, \dots, \mathbf{x}_{\lambda:\lambda}\}$ and $\{\mathbf{y}_{1:\lambda}, \mathbf{y}_{2:\lambda}, \dots, \mathbf{y}_{\lambda:\lambda}\}$ so that the indices correspond to $f(\bar{\mathbf{v}}_{1:\lambda}) \leq f(\bar{\mathbf{v}}_{2:\lambda}) \leq \dots \leq f(\bar{\mathbf{v}}_{\lambda:\lambda})$.
- Step 4. Based on (3) to (7), update $\mathbf{m}^{(t)}$, $\mathbf{C}^{(t)}$, and $\sigma^{(t)}$ using \mathbf{x} and \mathbf{y} .
- Step 5. Modify $\mathbf{m}^{(t+1)}$ and update $\mathbf{A}^{(t)}$ based on Section 4.3 and Section 4.4.

It should be noted that the algorithm based on the above is consistent with the original CMA-ES if no corrections are made in Step 5. In other words, the smaller the margin parameter α , described in Section 4.3 and Section 4.4, and the more insignificant the modification, the closer the above algorithm is to the original CMA-ES. Moreover, the update of the variance-covariance has not been modified, which facilitates the smooth consideration of the introduction of the CMA-ES properties, e.g., step-size adaptation methods other than CSA.

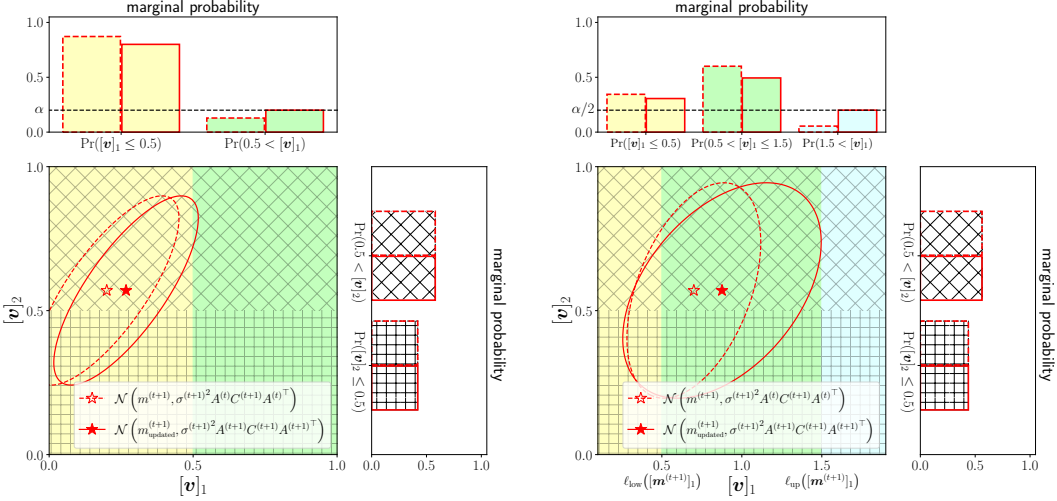


Fig. 2. Example of MGD followed by ν and its marginal probability. The dashed red ellipse corresponds to the MGD before the correction, whereas the solid one corresponds to the MGD after the correction for the binary variable (left) and for the integer variable (right).

4.3 Margin for Binary Variables

Considering the probability that a binarized variable $[\bar{v}]_j$ is 0 and the probability that it is 1, the following conditions should be satisfied after the modification by the margin:

$$\min \{\Pr([\bar{v}]_j = 0), \Pr([\bar{v}]_j = 1)\} \geq \alpha \Leftrightarrow \min \{\Pr([\bar{v}]_j < 0.5), \Pr([\bar{v}]_j \geq 0.5)\} \geq \alpha \quad (12)$$

It should be noted that the binarize threshold $\ell_{j,1|2}$ is equal to 0.5. Here, the left of Figure 2 shows an example of the updated MGD followed by ν and the marginal probabilities. The MGD before the margin correction (dashed red ellipse) shows that its marginal probability $\Pr([\bar{v}]_1 \geq 0.5)$ is smaller than the margin parameter α . In this case, by modifying the element of the mean vector $[\mathbf{m}^{(t+1)}]_1$, we can correct the marginal probability $\Pr([\bar{v}]_1 \geq 0.5)$ to α without affecting the other dimensions. To calculate the amount of the correction for this mean vector, we consider the confidence interval of the probability $1 - 2\alpha$ in the marginal distribution of the j -th dimension. The confidence interval of the j -th dimension is represented by

$$[\mathbf{m}^{(t+1)}]_j - \text{CI}_j^{(t+1)}(1 - 2\alpha), [\mathbf{m}^{(t+1)}]_j + \text{CI}_j^{(t+1)}(1 - 2\alpha) \quad .$$

It should be noted that $\text{CI}_j^{(t+1)}(1 - 2\alpha)$ is defined as

$$\text{CI}_j^{(t+1)}(1 - 2\alpha) := \sqrt{\chi_{\text{ppf}}^2(1 - 2\alpha) \sigma^{(t+1)2} \langle \mathbf{A}^{(t)} \mathbf{C}^{(t+1)} \mathbf{A}^{(t)\top} \rangle_j} \quad ,$$

where $\chi_{\text{ppf}}^2(\cdot)$ is the function that, given the lower cumulative probability, returns the percentage point in the chi-squared distribution with 1 degree of freedom. If the threshold $\ell_{j,1|2} = 0.5$ is outside this confidence interval, the marginal probability to be corrected is less than α . Given the encoding threshold closest to $[\mathbf{m}^{(t+1)}]_j$ as $\ell([\mathbf{m}^{(t+1)}]_j)$, which is

equal to 0.5 in the binary case, the modification for the j -th element of the mean vector can be denoted as

$$[\mathbf{m}^{(t+1)}]_j \leftarrow \ell([\mathbf{m}^{(t+1)}]_j) + \text{sign}([\mathbf{m}^{(t+1)}]_j - \ell([\mathbf{m}^{(t+1)}]_j)) \cdot \min \left\{ \left| [\mathbf{m}^{(t+1)}]_j - \ell([\mathbf{m}^{(t+1)}]_j) \right|, \text{CI}_j^{(t+1)}(1 - 2\alpha) \right\} . \quad (13)$$

Additionally, no changes are made to $\langle \mathbf{A}^{(t)} \rangle_j$, namely,

$$\langle \mathbf{A}^{(t+1)} \rangle_j \leftarrow \langle \mathbf{A}^{(t)} \rangle_j . \quad (14)$$

As shown in the solid red line in the left of Figure 2, the marginal probability after this modification is lower-bounded by α .

4.4 Margin for Integer Variables

First, we consider the cases where the j -th element of the mean vector satisfies $[\mathbf{m}^{(t+1)}]_j \leq \ell_{j,1|2}$ or $\ell_{j,K_j-1|K_j} < [\mathbf{m}^{(t+1)}]_j$. In these cases, the integer variable $[\mathbf{v}]_j$ may be fixed to $z_{j,1}$ or z_{j,K_j} , respectively. Thus, we correct the marginal probability of generating one inner integer variable, i.e., $z_{j,2}$ for $z_{j,1}$ or z_{j,K_j-1} for z_{j,K_j} , to maintain it above α , respectively. This correction is achieved by updating $[\mathbf{m}^{(t+1)}]_j$ and $\mathbf{A}^{(t)}$ based on (13) and (14).

Next, we consider the case of other integer variables. The right of Figure 2 shows an example of the updated MGD followed by \mathbf{v} and the marginal probability. In this example, $[\mathbf{v}]_1$ is expected to be fixed in the interval $(0.5, 1.5]$ when $\Pr([\mathbf{v}]_1 \leq 0.5)$ and $\Pr(1.5 < [\mathbf{v}]_1)$ become small. Thus, the correction strategy is to lower-bound the probability of $[\mathbf{v}]_j$ being generated outside the plateau where $[\mathbf{v}]_j$ is expected to be fixed, such as $\Pr([\mathbf{v}]_1 \leq 0.5)$ and $\Pr(1.5 < [\mathbf{v}]_1)$ in the right of Figure 2. In this case, the value of the margin is set to $\alpha/2$. For simplicity, we denote $\ell_{\text{low}}([\mathbf{m}^{(t+1)}]_j)$ and $\ell_{\text{up}}([\mathbf{m}^{(t+1)}]_j)$ as

$$\ell_{\text{low}}([\mathbf{m}^{(t+1)}]_j) := \max \left\{ l \in \ell_j : l < [\mathbf{m}^{(t+1)}]_j \right\} , \quad (15)$$

$$\ell_{\text{up}}([\mathbf{m}^{(t+1)}]_j) := \min \left\{ l \in \ell_j : [\mathbf{m}^{(t+1)}]_j \leq l \right\} . \quad (16)$$

The first step of the modification is to calculate p_{low} , p_{up} , and p_{mid} as follows.

$$p_{\text{low}} \leftarrow \Pr \left([\mathbf{v}]_j \leq \ell_{\text{low}}([\mathbf{m}^{(t+1)}]_j) \right) \quad (17)$$

$$p_{\text{up}} \leftarrow \Pr \left(\ell_{\text{up}}([\mathbf{m}^{(t+1)}]_j) < [\mathbf{v}]_j \right) \quad (18)$$

$$p_{\text{mid}} \leftarrow 1 - p_{\text{low}} - p_{\text{up}} \quad (19)$$

Next, we restrict p_{low} , p_{up} , and p_{mid} as follows.

$$p'_{\text{low}} \leftarrow \max \{ \alpha/2, p_{\text{low}} \} \quad (20)$$

$$p'_{\text{up}} \leftarrow \max \{ \alpha/2, p_{\text{up}} \} \quad (21)$$

$$p''_{\text{low}} \leftarrow p'_{\text{low}} + \frac{1 - p'_{\text{low}} - p'_{\text{up}} - p_{\text{mid}}}{p'_{\text{low}} + p'_{\text{up}} + p_{\text{mid}} - 3 \cdot \alpha/2} (p'_{\text{low}} - \alpha/2) \quad (22)$$

$$p''_{\text{up}} \leftarrow p'_{\text{up}} + \frac{1 - p'_{\text{low}} - p'_{\text{up}} - p_{\text{mid}}}{p'_{\text{low}} + p'_{\text{up}} + p_{\text{mid}} - 3 \cdot \alpha/2} (p'_{\text{up}} - \alpha/2) \quad (23)$$

The equations (22) and (23) ensure $p''_{\text{low}} + p''_{\text{up}} + p'_{\text{mid}} = 1$, while keeping $p''_{\text{low}} \geq \alpha/2$ and $p''_{\text{up}} \geq \alpha/2$, where $p'_{\text{mid}} = 1 - p''_{\text{low}} - p''_{\text{up}}$. This handling method is also adopted in [Akimoto et al. 2019, Appendix D]. We update $\mathbf{m}^{(t+1)}$ and $\mathbf{A}^{(t)}$

so that the corrected marginal probabilities $\Pr([v]_j \leq \ell_{\text{low}}([\mathbf{m}^{(t+1)}]_j))$ and $\Pr(\ell_{\text{up}}([\mathbf{m}^{(t+1)}]_j) < [v]_j)$ are p_{low}'' and p_{up}'' , respectively. The conditions to be satisfied are as follows.

$$\begin{cases} [\mathbf{m}^{(t+1)}]_j - \ell_{\text{low}}([\mathbf{m}^{(t+1)}]_j) = \text{CI}_j^{(t+1)}(1 - 2p_{\text{low}}'') \\ \ell_{\text{up}}([\mathbf{m}^{(t+1)}]_j) - [\mathbf{m}^{(t+1)}]_j = \text{CI}_j^{(t+1)}(1 - 2p_{\text{up}}'') \end{cases} \quad (24)$$

Finally, the solutions of the simultaneous linear equations for $[\mathbf{m}^{(t+1)}]_j$ and $\langle \mathbf{A}^{(t)} \rangle_j$ are applied to the updated $[\mathbf{m}^{(t+1)}]_j$ and $\langle \mathbf{A}^{(t+1)} \rangle_j$ as follows:

$$[\mathbf{m}^{(t+1)}]_j \leftarrow \frac{\ell_{\text{low}}([\mathbf{m}^{(t+1)}]_j) \sqrt{\chi_{\text{ppf}}^2(1 - 2p_{\text{up}}'')} + \ell_{\text{up}}([\mathbf{m}^{(t+1)}]_j) \sqrt{\chi_{\text{ppf}}^2(1 - 2p_{\text{low}}'')}}{\sqrt{\chi_{\text{ppf}}^2(1 - 2p_{\text{low}}'')} + \sqrt{\chi_{\text{ppf}}^2(1 - 2p_{\text{up}}'')}} \quad (25)$$

$$\langle \mathbf{A}^{(t+1)} \rangle_j \leftarrow \frac{\ell_{\text{up}}([\mathbf{m}^{(t+1)}]_j) - \ell_{\text{low}}([\mathbf{m}^{(t+1)}]_j)}{\sigma^{(t+1)} \sqrt{\langle \mathbf{C}^{(t+1)} \rangle_j} \left(\sqrt{\chi_{\text{ppf}}^2(1 - 2p_{\text{low}}'')} + \sqrt{\chi_{\text{ppf}}^2(1 - 2p_{\text{up}}'')} \right)} \quad (26)$$

Correcting $\mathbf{m}^{(t+1)}$ and $\mathbf{A}^{(t)}$ in this way bounds both $\Pr([v]_j \leq \ell_{\text{low}}([\mathbf{m}^{(t+1)}]_j))$ and $\Pr(\ell_{\text{up}}([\mathbf{m}^{(t+1)}]_j) < [v]_j)$ above $\alpha/2$, as indicated by the solid line in the right of Figure 2. Moreover, we note that there are cases where $p_{\text{mid}} \Pr(0.5 < [\mathbf{m}^{(t+1)}]_1 \leq 1.5)$ in the right of Figure 2, is less than $\alpha/2$ even with the margin. In that case, the variance is sufficiently large that no fixation of the discrete variable occurs in the corresponding dimension. Finally, we show the algorithm details in Algorithm 1, and the margin correction therein is described in Algorithm 2.

Algorithm 1: Single update in CMA-ES with Margin for optimization problem $\min_{\mathbf{x}} f(\mathbf{x})$

```

1: given  $\mathbf{m}^{(t)} \in \mathbb{R}^N$ ,  $\sigma^{(t)} \in \mathbb{R}_+$ ,  $\mathbf{C}^{(t)} \in \mathbb{R}^{N \times N}$ ,  $\mathbf{p}_\sigma^{(t)} \in \mathbb{R}^N$ ,  $\mathbf{p}_c^{(t)} \in \mathbb{R}^N$ , and  $\mathbf{A}^{(t)} \in \mathbb{R}^{N \times N}$  (diagonal matrix)
2: for  $i = 1, \dots, \lambda$  do
3:    $\mathbf{y}_i \sim \mathcal{N}(\mathbf{0}, \mathbf{C}^{(t)})$ 
4:    $\mathbf{x}_i \leftarrow \mathbf{m}^{(t)} + \sigma^{(t)} \mathbf{y}_i$ 
5:    $\mathbf{v}_i \leftarrow \mathbf{m}^{(t)} + \sigma^{(t)} \mathbf{A}^{(t)} \mathbf{y}_i^\top$ 
6:    $\bar{\mathbf{v}}_i \leftarrow \text{ENCODING}_f(\mathbf{v}_i)$ 
7: end for
8: Sort  $\{\mathbf{x}_{1:\lambda}, \mathbf{x}_{2:\lambda}, \dots, \mathbf{x}_{\lambda:\lambda}\}$  and  $\{\mathbf{y}_{1:\lambda}, \mathbf{y}_{2:\lambda}, \dots, \mathbf{y}_{\lambda:\lambda}\}$  so that the indices correspond to
    $f(\bar{\mathbf{v}}_{1:\lambda}) \leq f(\bar{\mathbf{v}}_{2:\lambda}) \leq \dots \leq f(\bar{\mathbf{v}}_{\lambda:\lambda})$ 
9:  $\mathbf{m}^{(t+1)} \leftarrow \mathbf{m}^{(t)} + c_m \sum_{i=1}^{\mu} \mathbf{w}_i (\mathbf{x}_{i:\lambda} - \mathbf{m}^{(t)})$ 
10:  $\mathbf{p}_\sigma^{(t+1)} \leftarrow (1 - c_\sigma) \mathbf{p}_\sigma^{(t)} + \sqrt{c_\sigma(2 - c_\sigma) \mu_w} \mathbf{C}^{(t)} \leftarrow \frac{1}{2} \sum_{i=1}^{\mu} \mathbf{w}_i \mathbf{y}_{i:\lambda}$ 
11:  $h_\sigma \leftarrow \mathbb{1}\{\|\mathbf{p}_\sigma^{(t+1)}\| < \sqrt{1 - (1 - c_\sigma)^2(t+1)} \left( 1.4 + \frac{2}{N+1} \right) \mathbb{E}[\|\mathcal{N}(\mathbf{0}, \mathbf{I})\|]\}$ 
12:  $\mathbf{p}_c^{(t+1)} \leftarrow (1 - c_c) \mathbf{p}_c^{(t)} + h_\sigma \sqrt{c_c(2 - c_c) \mu_w} \sum_{i=1}^{\mu} \mathbf{w}_i \mathbf{y}_{i:\lambda}$ 
13:  $\mathbf{C}^{(t+1)} \leftarrow \left( 1 - c_1 - c_\mu \sum_{i=1}^{\lambda} \mathbf{w}_i + (1 - h_\sigma) c_1 c_c (2 - c_c) \right) \mathbf{C}^{(t)} + \underbrace{c_1 \mathbf{p}_c^{(t+1)} \mathbf{p}_c^{(t+1)\top}}_{\text{rank-one update}} + \underbrace{c_\mu \sum_{i=1}^{\lambda} \mathbf{w}_i^\top \mathbf{y}_{i:\lambda} \mathbf{y}_{i:\lambda}^\top}_{\text{rank-}\mu\text{ update}}$ 
14:  $\sigma^{(t+1)} \leftarrow \sigma^{(t)} \exp \left( \frac{c_\sigma}{d_\sigma} \left( \frac{\|\mathbf{p}_\sigma^{(t+1)}\|}{\mathbb{E}[\|\mathcal{N}(\mathbf{0}, \mathbf{I})\|]} - 1 \right) \right)$ 
15:  $\mathbf{m}^{(t+1)}, \mathbf{A}^{(t+1)} \leftarrow \text{MarginCorrection}(\mathbf{m}^{(t+1)}, \mathbf{A}^{(t)}, \sigma^{(t+1)}, \mathbf{C}^{(t+1)})$ 

```

Algorithm 2: Margin Correction

```

1: given  $\mathbf{m} \in \mathbb{R}^N$ ,  $\mathbf{A} \in \mathbb{R}^{N \times N}$  (diagonal matrix),  $\sigma \in \mathbb{R}_+$ , and  $\mathbf{C} \in \mathbb{R}^{N \times N}$ 
2: // Margin for Continuous Variables (identity mapping)
3: for  $j = 1, \dots, N_{\text{co}}$  do
4:    $[\mathbf{m}']_j \leftarrow [\mathbf{m}]_j$ 
5:    $\langle \mathbf{A}' \rangle_j \leftarrow \langle \mathbf{A} \rangle_j$ 
6: end for
7: // Margin for Binary Variables
8: for  $j = N_{\text{co}} + 1, \dots, N_{\text{co}} + N_{\text{bi}}$  do
9:    $[\mathbf{m}]_j \leftarrow \ell([\mathbf{m}]_j) + \text{sign}([\mathbf{m}']_j - \ell([\mathbf{m}]_j)) \min \left\{ |[\mathbf{m}]_j - \ell([\mathbf{m}]_j)|, \text{CI}_j^{(t+1)}(1 - 2\alpha) \right\}$ 
10:   $\langle \mathbf{A}' \rangle_j \leftarrow \langle \mathbf{A} \rangle_j$ 
11: end for
12: // Margin for Integer Variables
13: for  $j = N_{\text{co}} + N_{\text{bi}} + 1, \dots, N$  do
14:   if  $[\mathbf{m}]_j \leq \ell_{j,1|2}$  or  $\ell_{j,K_j-1|K_j} < [\mathbf{m}]_j$  then
15:      $[\mathbf{m}']_j \leftarrow \ell([\mathbf{m}]_j) + \text{sign}([\mathbf{m}]_j - \ell([\mathbf{m}]_j)) \min \left\{ |[\mathbf{m}]_j - \ell([\mathbf{m}]_j)|, \text{CI}_j^{(t+1)}(1 - 2\alpha) \right\}$ 
16:      $\langle \mathbf{A}' \rangle_j \leftarrow \langle \mathbf{A} \rangle_j$ 
17:   else
18:      $[\mathbf{m}']_j \leftarrow \frac{\ell_{\text{low}}([\mathbf{m}]_j) \sqrt{\chi_{\text{ppf}}^2(1-2p_{\text{up}}'')} + \ell_{\text{up}}([\mathbf{m}]_j) \sqrt{\chi_{\text{ppf}}^2(1-2p_{\text{low}}'')}}{\sqrt{\chi_{\text{ppf}}^2(1-2p_{\text{low}}'')} + \sqrt{\chi_{\text{ppf}}^2(1-2p_{\text{up}}'')}}$ 
19:      $\langle \mathbf{A}' \rangle_j \leftarrow \frac{\ell_{\text{up}}([\mathbf{m}]_j) - \ell_{\text{low}}([\mathbf{m}]_j)}{\sigma^{(t+1)} \sqrt{\langle \mathbf{C}^{(t+1)} \rangle_j} \left( \sqrt{\chi_{\text{ppf}}^2(1-2p_{\text{low}}'')} + \sqrt{\chi_{\text{ppf}}^2(1-2p_{\text{up}}'')} \right)}$ 
20:   end if
21: end for
22: return  $\mathbf{m}'$  and  $\mathbf{A}'$ 

```

5 EXPERIMENT AND RESULT

We apply the proposed method to the MI-BBO optimization problem for several benchmark functions to validate its robustness and efficiency. In Section 5.1, we check the performance changes of the proposed method according to the hyperparameter α . In Section 5.2, we check the difference in the search success rate and the number of evaluations between the proposed method and CMA-ES-IM for several artificial MI-BBO benchmark functions. The definitions of the benchmark functions used in this section are listed as below:

- SPHEREONEMAX(\bar{x}) = $\sum_{j=1}^{N_{\text{co}}} [\bar{x}]_j^2 + N_{\text{bi}} - \sum_{k=N_{\text{co}}+1}^N [\bar{x}]_k$
- SPHERELEADINGONES(\bar{x}) = $\sum_{j=1}^{N_{\text{co}}} [\bar{x}]_j^2 + N_{\text{bi}} - \sum_{k=N_{\text{co}}+1}^N \prod_{l=N_{\text{co}}+1}^k [\bar{x}]_l$
- ELLIPSOIDONEMAX(\bar{x}) = $\sum_{j=1}^{N_{\text{co}}} \left(1000^{\frac{j-1}{N_{\text{co}}-1}} [\bar{x}]_j \right)^2 + N_{\text{bi}} - \sum_{k=N_{\text{co}}+1}^N [\bar{x}]_k$
- ELLIPSOIDLEADINGONES(\bar{x}) = $\sum_{j=1}^{N_{\text{co}}} \left(1000^{\frac{j-1}{N_{\text{co}}-1}} [\bar{x}]_j \right)^2 + N_{\text{bi}} - \sum_{k=N_{\text{co}}+1}^N \prod_{l=N_{\text{co}}+1}^k [\bar{x}]_l$
- SPHEREINT(\bar{x}) = $\sum_{j=1}^N [\bar{x}]_j^2$
- ELLIPSOIDINT(\bar{x}) = $\sum_{j=1}^N \left(1000^{\frac{j-1}{N-1}} [\bar{x}]_j \right)^2$

In all functions, the first N_{co} variables are continuous, whereas the last $N - N_{\text{co}}$ variables are binary or integer. In all the experiments, we adopted the default parameters of the CMA-ES listed in Table 1.

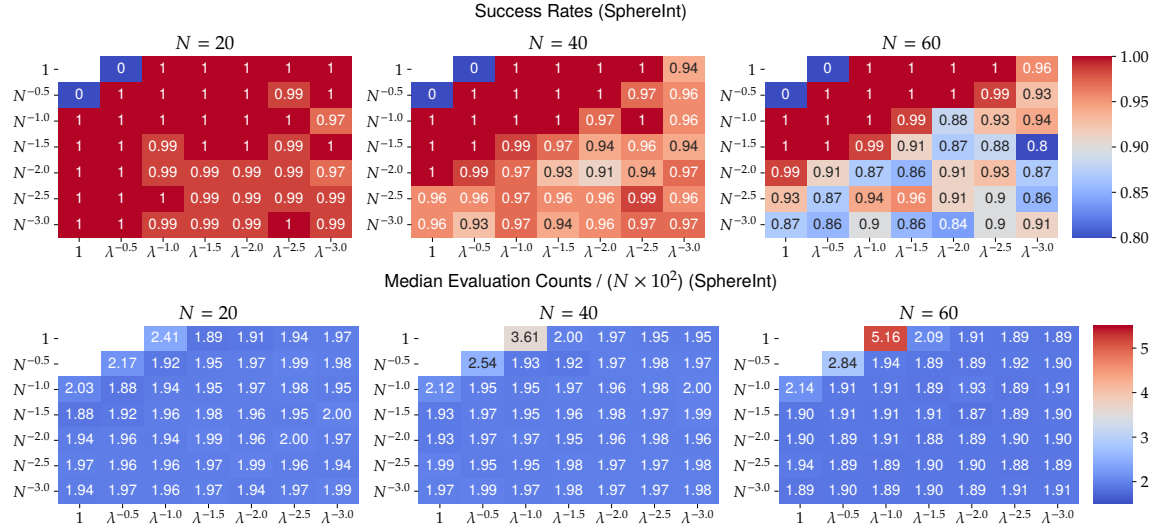


Fig. 3. Heatmap of the success rate (top) and the median evaluation counts for successful cases (bottom) in the N -dimensional SPHEREINT function when the hyperparameter $\alpha = N^{-m}\lambda^{-n}$ of the proposed method is changed.

Table 2. Comparison of evaluation counts and success rate for the benchmark functions. The evaluation counts are reported as the median value of successful trials. The bold fonts represent the best median evaluation counts and the best success rates among the methods. The inside of the parentheses represents the interquartile range (IQR).

Function	N	CMA-ES-IM		CMA-ES-IM & Box-constraint		CMA-ES w. Margin (Proposed)	
		Evaluation Counts	Success Rates	Evaluation Counts	Success Rates	Evaluation Counts	Success Rates
SPHEREONEMAX	20	2964 (174)	83/100	4752 (100)	100/100	3876 (435)	100/100
	40	5745 (558)	62/100	7575 (543)	64/100	7995 (514)	100/100
	60	8112 (340)	46/100	12240 (336)	21/100	12408 (1012)	100/100
SPHERELEADINGONES	20	2904 (192)	77/100	5124 (296)	100/100	4158 (339)	100/100
	40	5647 (296)	24/100	8280 (112)	10/100	8505 (724)	100/100
	60	8816 (12)	8/100	12624 (96)	2/100	13424 (1008)	100/100
ELLIPSOIDONEMAX	20	9918 (396)	20/100	26700 (7020)	96/100	11172 (666)	100/100
	40	35325 (0)	1/100	79912 (28661)	14/100	40590 (1789)	100/100
	60	78560 (0)	5/100	283440 (0)	1/100	88064 (3536)	100/100
ELLIPSOIDLEADINGONES	20	10104 (441)	14/100	24880 (7305)	92/100	11454 (876)	100/100
	40	-	0/100	85807 (13335)	4/100	41048 (1744)	100/100
	60	-	0/100	-	0/100	91496 (3488)	100/100
SPHEREINT	20	5130 (477)	86/100	5280 (744)	89/100	3840 (306)	100/100
	40	7950 (697)	71/100	8070 (555)	85/100	7838 (458)	100/100
	60	13184 (816)	41/100	12992 (544)	34/100	11512 (544)	100/100
ELLIPSOIDINT	20	19128 (3192)	76/100	19476 (5028)	73/100	8418 (837)	100/100
	40	43935 (4095)	73/100	43440 (4762)	83/100	22815 (1733)	100/100
	60	89200 (6152)	54/100	86848 (6136)	54/100	42000 (3320)	100/100

5.1 Hyperparameter Sensitivity for α

We use the SPHEREINT function of the objective function and adopt the same initialization for the distribution parameters and termination condition as in Section 3. The number of dimensions N is set to 20, 40, or 60, and the numbers of the continuous and integer variables are $N_{\text{co}} = N_{\text{int}} = N/2$. The integer variables are assumed to take values in the range $[-10, 10]$. We argue that it is reasonable that the hyperparameter α , which determines the margin in the proposed method, should depend on the number of dimensions N and the sample size λ . In this experiment, we evaluate a total of 48 settings except for $\alpha = 1$ which we set as $\alpha = N^{-m}\lambda^{-n}$ ($m, n \in [0, 0.5, 1, 1.5, 2, 2.5, 3]$). In each setting, 100 trials are performed independently using different seed values.

Results and Discussion. Figure 3 shows the success rate and the median evaluation count for successful cases in each setting. For the success rate, when α is set to a large value as $N^{-0.5}$ or $\lambda^{-0.5}$, all trials fail. Additionally, when α is set as smaller than $(N\lambda)^{-1}$, the success rate tends to decrease as the number of dimensions N increases. If α is too large, the probability of the integer changing is also too large and the optimization is unstable; however, if α is too small, it is difficult to get out of the stagnation because the conditions under which the mean $[\mathbf{m}]_j$ and affine matrix \mathbf{A} corrections are applied become more stringent. For the median evaluation count, there is no significant difference for any dimension except for $\alpha = N^{-1}, (N\lambda)^{-0.5}, \lambda^{-1}$. Therefore, for robustness and efficiency reasons, we use $\alpha = (N\lambda)^{-1}$ as a default parameter in the subsequent experiments in this study.

5.2 Comparison of Optimization Performance

We compare the optimization performance of the benchmark functions listed in Section 5 for the proposed method, CMA-ES-IM, and CMA-ES-IM with box constraints. As in Section 5.1, the number of dimensions N is set to 20, 40, and 60. The number of continuous and integer variables are $N_{\text{co}} = N_{\text{bi}} = N_{\text{int}} = N/2$, respectively. For CMA-ES-IM with the box constraint, SPHEREONEMAX, SPHERELEADINGONES, ELLIPSOIDONEMAX, and ELLIPSOIDLEADINGONES functions are given the constraint $[x]_j \in [-1, 1]$ corresponding to the binary variables, and other functions are given the constraint $[x]_j \in [-10, 10]$ corresponding to the integer variables. The calculating method of the penalty for violating the constraints is the same as in Section 3. The optimization is successful when the best-evaluated value is less than 10^{-10} , whereas the optimization is stopped when the minimum eigenvalue of $\sigma^2 \mathbf{C}$ is less than 10^{-30} or the condition number of \mathbf{C} exceeds 10^{14} .

Results and Discussion. Table 2 summarizes the median evaluation counts and success rates in each setting. Comparing the proposed method with the CMA-ES-IM with and without the box constraint for the SPHEREONEMAX and SPHERELEADINGONES functions, the CMA-ES-IM reaches the optimal solution in fewer evaluation counts. However, the success rate of CMA-ES-IM with and without the box constraint decreases as the number of dimensions increases. However, the success rate of the proposed method remains 100% regardless of the increase in the number of dimensions. For the ELLIPSOIDONEMAX and ELLIPSOIDLEADINGONES functions, the CMA-ES-IM without the box constraint fails on most of the trials in all dimensions, and the CMA-ES-IM with box constraint has a relatively high success rate in $N = 20$ but deteriorates rapidly in $N = 40$ or more dimensions. In contrast, the proposed method maintains a 100% success rate and reaches the optimal solution in fewer evaluation counts than the CMA-ES-IM with the box constraint in $N = 20, 40$. For the SPHEREINT and ELLIPSOIDINT functions, the proposed method successfully optimizes with fewer evaluations in all dimensions than the other methods, maintaining a 100% success rate. These results show that the proposed method can perform the MI-BBO robustly and efficiently for multiple functions with an increasing number of dimensions.

6 EXTENSION TO MULTI-OBJECTIVE OPTIMIZATION

In this section, we present the application of the margin correction to multi-objective mixed-integer black-box optimization (MO-MI-BBO). First, we briefly review the MO-MI-BBO and the MO-CMA-ES, followed by a discussion of the introduction of the margin into the MO-CMA-ES.

6.1 Multi-Objective Mixed-Integer Optimization

A multi-objective optimization problem is an optimization problem that targets multiple objective functions. In this paper, we will consider multi-objective optimization involving continuous and integer variables and refer to it as multi-objective mixed-integer optimization (MO-MI-BBO). The M -objective MO-MI-BBO is formally defined as follows:

$$\begin{aligned} & \underset{\mathbf{x}}{\text{minimize}} \quad (f_1(\mathbf{x}), \dots, f_M(\mathbf{x})) \\ & \text{where } f_m : \mathbb{R}^{N_{\text{co}}} \times \{0, 1\}^{N_{\text{bi}}} \times \mathbb{Z}^{N_{\text{in}}} \rightarrow \mathbb{R} \\ & N = N_{\text{co}} + N_{\text{bi}} + N_{\text{in}} \\ & x_i \in \{0, 1\} \quad \text{if } N_{\text{co}} + 1 \leq i \leq N_{\text{co}} + N_{\text{bi}} \\ & x_i \in [x_i^{\text{min}}, x_i^{\text{max}}] \cap \mathbb{Z} \quad \text{if } N_{\text{co}} + N_{\text{bi}} + 1 \leq i \leq N \end{aligned}$$

The goal of multi-objective optimization, including MO-MI-BBO, is to find a diverse set of Pareto-optimal solutions. The set of Pareto-optimal solutions is often evaluated by the hypervolume measure or \mathcal{S} -metric, which is defined as the Lebesgue measure of the union of hypercuboids in the objective space [Zitzler and Thiele 1998]. Multi-objective evolutionary algorithms often use this hypervolume measure and non-dominated sorting, as described below during the search.

6.2 MO-CMA-ES

The multi-objective covariance matrix adaptation strategy (MO-CMA-ES) [Igel et al. 2007] is an extension of the CMA-ES for multi-objective black-box optimization. It combines the strategy parameter adaptation of (1+1)-CMA-ES with multi-objective selection based on non-dominated sorting [Deb et al. 2002] and the contributing hypervolume [Emmerich et al. 2005]. In the MO-CMA-ES, step sizes are adapted to each individual in addition to the solution. Moreover, the success rule is applied to each pair of parent and offspring, and the mutation is regarded as successful if the offspring has a higher rank than the parent. In contrast, Voß et al. [Voß et al. 2010] proposed a new update scheme for the MO-CMA-ES, which considers a mutation successful if the offspring are selected for the next parent population. This significantly improved performance in the MO-CMA-ES by avoiding premature convergence of the step size. In this paper, we focus on this improved MO-CMA-ES as a baseline. For simplicity, we consider the case $\mu = \lambda$, where the number of parent and offspring individuals is equal. When applying the improved MO-CMA-ES to MO-MI-BBO, we repeat the following steps until a termination criterion is satisfied.

Notation. The improved MO-CMA-ES denotes the i -th individual $\mathbf{a}_i^{(t)}$ in generation t by the tuple $\left[\mathbf{x}_i^{(t)}, \bar{\mathbf{v}}_i^{(t)}, \bar{p}_{\text{succ},i}^{(t)}, \sigma_i^{(t)}, \mathbf{p}_{c,i}^{(t)}, C_i^{(t)} \right]$, where $\mathbf{x}_i^{(t)}$ is the search point, $\bar{\mathbf{v}}_i^{(t)}$ is the discretized search point, $\bar{p}_{\text{succ},i}^{(t)}$ is the success probability, $\sigma_i^{(t)}$ is the global step size, $\mathbf{p}_{c,i}^{(t)}$ is the evolution path, $C_i^{(t)}$ is the covariance matrix of the search distribution.

Sample Offspring individuals. In the t -th iteration, each of the λ offspring individuals $\mathbf{a}'_i^{(t+1)}$ ($i = 1, \dots, \lambda$) is copied from its parent $\mathbf{a}_i^{(t)}$. Then mutate $\mathbf{x}'_i^{(t+1)}$ according to $\sigma_i^{(t)}$ and $C_i^{(t)}$ as follows.

$$\mathbf{x}'_i^{(t+1)} \sim \mathbf{x}_i^{(t)} + \sigma_i^{(t)} \mathcal{N}(\mathbf{0}, C_i^{(t)}) \quad (27)$$

Moreover, the discretized search point $\bar{\mathbf{v}}_i^{(t+1)}$ is calculated using ENCODING_f introduced in Section 4.1.

$$\bar{\mathbf{v}}_i^{(t+1)} = \text{ENCODING}_f(\mathbf{x}'_i^{(t+1)}) \quad (28)$$

Ranking the individuals. Rank the individuals in the set of parent and offspring individuals $Q^{(t)}$ based on the non-dominated sorting and the contributing hypervolume. For details, see [Voß et al. 2010, Equation 5]. However, note that in the case of MO-MI-BBO, the argument of the objective function is not $\mathbf{x}_i^{(t)}$ but $\bar{\mathbf{v}}_i^{(t)}$, i.e., $f_m(\mathbf{a}_i^{(t)})$ implies $f_m(\bar{\mathbf{v}}_i^{(t)})$, not $f_m(\mathbf{x}_i^{(t)})$. The i -th best individual ranked by non-domain sorting and the contributing hypervolume in $Q^{(t)}$ is defined as $Q_{\leq i}^{(t)}$. Then, the next parent population is denoted by $Q^{(t+1)} = \{Q_{\leq i}^{(t)} \mid 1 \leq i \leq \lambda\}$ since the top λ individuals are selected from $Q^{(t)}$.

Success Indicator. In the MO-CMA-ES, the step size and covariance matrix are updated based on the success rule. The success of the mutation from parent individual $\mathbf{a}_i^{(t)}$ to offspring individual $\mathbf{a}'_i^{(t+1)}$ is determined by whether the offspring individual $\mathbf{a}'_i^{(t+1)}$ is selected for the next parent population $Q^{(t+1)}$, i.e., the success indicator $\text{succ}_{Q^{(t)}}(\mathbf{a}_i^{(t)}, \mathbf{a}'_i^{(t+1)})$ is defined by

$$\text{succ}_{Q^{(t)}}(\mathbf{a}_i^{(t)}, \mathbf{a}'_i^{(t+1)}) = \begin{cases} 1 & \text{if } \mathbf{a}'_i^{(t+1)} \in Q^{(t+1)} \\ 0 & \text{otherwise} \end{cases} \quad (29)$$

Compute Success Probabilities and Step-Size Adaptation. The smoothed success probabilities are calculated as

$$\bar{p}'_{\text{succ},i}^{(t+1)} = (1 - c_p) \bar{p}'_{\text{succ},i}^{(t+1)} + c_p \text{succ}_{Q^{(t)}}(\mathbf{a}_i^{(t)}, \mathbf{a}'_i^{(t+1)}) \quad (30)$$

where c_p is the success rate averaging parameter. According to each success probability, step-size adaptation is performed as

$$\sigma'_i^{(t+1)} = \sigma_i^{(t+1)} \exp\left(\frac{1}{d} \frac{\bar{p}'_{\text{succ},i}^{(t+1)} - p_{\text{succ}}^{\text{target}}}{1 - p_{\text{succ}}^{\text{target}}}\right), \quad (31)$$

where $p_{\text{succ}}^{\text{target}}$ is the target success probability.

Update Covariance Matrix and Evolution Path. Based on the success probability $\bar{p}'_{\text{succ},i}^{(t+1)}$, the evolution path $\mathbf{p}'_{c,i}^{(t+1)}$ and covariance matrix $C'_i^{(t+1)}$ are updated. If $\bar{p}'_{\text{succ},i}^{(t+1)} < p_{\text{thresh}}$,

$$\mathbf{p}'_{c,i}^{(t+1)} = (1 - c_c) \mathbf{p}'_{c,i}^{(t+1)} + \sqrt{c_c(2 - c_c)} \frac{\mathbf{x}'_i^{(t+1)} - \mathbf{x}^{(t)}}{\sigma_i^{(t)}} \quad (32)$$

$$C'_i^{(t+1)} = (1 - c_{\text{cov}}) C'_i^{(t+1)} + c_{\text{cov}} \mathbf{p}'_{c,i}^{(t+1)} \mathbf{p}'_{c,i}^{(t+1)\top} \quad (33)$$

If $\bar{p}'_{\text{succ},i}^{(t+1)} \geq p_{\text{thresh}}$,

$$\mathbf{p}'_{c,i}^{(t+1)} = (1 - c_c) \mathbf{p}'_{c,i}^{(t+1)} , \quad (34)$$

$$\mathbf{C}'_i^{(t+1)} = (1 - c_{\text{cov}}) \mathbf{C}'_i^{(t+1)} + c_{\text{cov}} \left(\mathbf{p}'_{c,i}^{(t+1)} \mathbf{p}'_{c,i}^{(t+1)\top} + c_c (2 - c_c) \mathbf{C}'_i^{(t+1)} \right) . \quad (35)$$

Update Parent individuals. The success probability $\bar{p}_{\text{succ},i}^{(t)}$ and step size $\sigma_i^{(t)}$ of the parent individuals $\mathbf{a}_i^{(t)}$ are adapted as follows.

$$\bar{p}_{\text{succ},i}^{(t)} = (1 - c_p) \bar{p}_{\text{succ},i}^{(t)} + c_p \text{succ}_{Q^{(t)}} \left(\mathbf{a}_i^{(t)}, \mathbf{a}'_i^{(t+1)} \right) \quad (36)$$

$$\sigma_i^{(t)} = \sigma_i^{(t)} \exp \left(\frac{1}{d} \frac{\bar{p}_{\text{succ},i}^{(t)} - p_{\text{succ}}^{\text{target}}}{1 - p_{\text{succ}}^{\text{target}}} \right) \quad (37)$$

Select New Parent Population. Finally, the new parent population is selected from the set of parent and offspring individuals. The top λ individuals are the parents of the next generation.

$$Q^{(t+1)} = \left\{ Q_{\leq i}^{(t)} \mid 1 \leq i \leq \lambda \right\} \quad (38)$$

6.3 Introduction of Margin to MO-CMA-ES

To address the fixation that can occur when the MO-CMA-ES is applied to MO-MI-BBO, we introduce the margin to MO-CMA-ES. In introducing the margin, there are two differences between the MO-CMA-ES and the single-objective CMA-ES introduced in Section 2. The first is that in the MO-CMA-ES, the step size and covariance are updated for each individual. Therefore, the matrix \mathbf{A} for margin correction should also be prepared for each individual, i.e., the tuple for the individual $\mathbf{a}_i^{(t)}$ is redefined as $[\mathbf{x}_i^{(t)}, \bar{v}_i^{(t)}, \bar{p}_{\text{succ},i}^{(t)}, \sigma_i^{(t)}, \mathbf{p}_{c,i}^{(t)}, \mathbf{C}_i^{(t)}, \mathbf{A}_i^{(t)}]$. The second is that the MO-CMA-ES uses an elitist evolution strategy, and the margin correction targets the search point $\mathbf{x}_i^{(t)}$. To discuss the validity of the margin correction in the elitist evolution strategy, we show that the discretized search points are invariant before and after the margin correction in the following proposition.

PROPOSITION 1. *Consider the margin correction for an individual $\mathbf{a}_i^{(t)}$. Let $\tilde{\mathbf{x}}_i^{(t)}$ be the margin-corrected search point. Then, it holds*

$$\text{ENCODING}_f(\mathbf{x}_i^{(t)}) = \text{ENCODING}_f(\tilde{\mathbf{x}}_i^{(t)}) \quad (39)$$

PROOF. We will show that it holds, for $j = 1, \dots, N$,

$$\text{ENCODING}_f([\mathbf{x}_i^{(t)}]_j) = \text{ENCODING}_f([\tilde{\mathbf{x}}_i^{(t)}]_j) . \quad (40)$$

First, when $j = 1, \dots, N_{\text{co}}$, it is obvious that (40) holds since $[\mathbf{x}_i^{(t)}]_j = [\tilde{\mathbf{x}}_i^{(t)}]_j$. Next, when $j = N_{\text{co}} + 1, \dots, N_{\text{co}} + N_{\text{bi}}$,

$$[\tilde{\mathbf{x}}_i^{(t)}]_j = \ell([\mathbf{x}_i^{(t)}]_j) + \text{sign}([\mathbf{x}_i^{(t)}]_j - \ell([\mathbf{x}_i^{(t)}]_j)) \min \left\{ \left| [\mathbf{x}_i^{(t)}]_j - \ell([\mathbf{x}_i^{(t)}]_j) \right|, \text{CI}_j^{(t)}(1 - 2\alpha) \right\} . \quad (41)$$

If $\ell([\mathbf{x}_i^{(t)}]_j) < [\mathbf{x}_i^{(t)}]_j$,

$$[\tilde{\mathbf{x}}_i^{(t)}]_j = \ell([\mathbf{x}_i^{(t)}]_j) + \min \left\{ \left| [\mathbf{x}_i^{(t)}]_j - \ell([\mathbf{x}_i^{(t)}]_j) \right|, \text{CI}_j^{(t)}(1 - 2\alpha) \right\} > \ell([\mathbf{x}_i^{(t)}]_j) . \quad (42)$$

$$\text{If } [\mathbf{x}_i^{(t)}]_j \leq \ell([\mathbf{x}_i^{(t)}]_j),$$

$$[\tilde{\mathbf{x}}_i^{(t)}]_j = \ell([\mathbf{x}_i^{(t)}]_j) - \min \left\{ \left| [\mathbf{x}_i^{(t)}]_j - \ell([\mathbf{x}_i^{(t)}]_j) \right|, \text{CI}_j^{(t)}(1 - 2\alpha) \right\} \leq \ell([\mathbf{x}_i^{(t)}]_j) . \quad (43)$$

Therefore, we have

$$\begin{cases} \ell([\mathbf{x}_i^{(t)}]_j) < [\tilde{\mathbf{x}}_i^{(t)}]_j & \text{if } \ell([\mathbf{x}_i^{(t)}]_j) < [\mathbf{x}_i^{(t)}]_j \\ [\tilde{\mathbf{x}}_i^{(t)}]_j \leq \ell([\mathbf{x}_i^{(t)}]_j) & \text{if } [\mathbf{x}_i^{(t)}]_j \leq \ell([\mathbf{x}_i^{(t)}]_j) \end{cases} , \quad (44)$$

which shows that (40) holds when $j = N_{\text{co}} + 1, \dots, N_{\text{co}} + N_{\text{bi}}$. Finally, when $j = N_{\text{co}} + N_{\text{bi}} + 1, \dots, N$,

$$[\tilde{\mathbf{x}}_i^{(t)}]_j = \frac{\ell_{\text{low}}([\mathbf{x}_i^{(t)}]_j) \sqrt{\chi_{\text{ppf}}^2(1 - 2p_{\text{up}}'')} + \ell_{\text{up}}([\mathbf{x}_i^{(t)}]_j) \sqrt{\chi_{\text{ppf}}^2(1 - 2p_{\text{low}}'')}}{\sqrt{\chi_{\text{ppf}}^2(1 - 2p_{\text{low}}'')} + \sqrt{\chi_{\text{ppf}}^2(1 - 2p_{\text{up}}'')}} \quad (45)$$

$$= \ell_{\text{low}}([\mathbf{x}_i^{(t)}]_j) + (\ell_{\text{up}}([\mathbf{x}_i^{(t)}]_j) - \ell_{\text{low}}([\mathbf{x}_i^{(t)}]_j)) \frac{\sqrt{\chi_{\text{ppf}}^2(1 - 2p_{\text{up}}'')}}{\sqrt{\chi_{\text{ppf}}^2(1 - 2p_{\text{up}}'')} + \sqrt{\chi_{\text{ppf}}^2(1 - 2p_{\text{low}}'')}} . \quad (46)$$

Since

$$0 < \frac{\sqrt{\chi_{\text{ppf}}^2(1 - 2p_{\text{up}}'')}}{\sqrt{\chi_{\text{ppf}}^2(1 - 2p_{\text{up}}'')} + \sqrt{\chi_{\text{ppf}}^2(1 - 2p_{\text{low}}'')}} < 1 , \quad (47)$$

we have

$$\ell_{\text{low}}([\mathbf{x}_i^{(t)}]_j) < [\tilde{\mathbf{x}}_i^{(t)}]_j < \ell_{\text{up}}([\mathbf{x}_i^{(t)}]_j) , \quad (48)$$

which shows that (40) holds when $j = N_{\text{co}} + N_{\text{bi}} + 1, \dots, N$. From the above, (40) holds when $j = 1, \dots, N$, and $\text{ENCODING}_f(\mathbf{x}_i^{(t)}) = \text{ENCODING}_f(\tilde{\mathbf{x}}_i^{(t)})$ holds. This is the end of the proof. \square

Proposition 1 shows that before and after the margin correction, the invariance of the discretized search points is preserved, and the evaluation values of each individual do not change. The ranking and contributing hypervolume of each individual also remain unchanged.

The single update in the MO-CMA-ES with margin is shown in Algorithm 3. See Algorithm 2 for the margin correction in lines 22 and 23. Shaded areas are modifications of the original improved MO-CMA-ES. If lines 6 and 7 are replaced by $\bar{\mathbf{v}}_i^{(t+1)} \leftarrow \text{ENCODING}_f(\mathbf{x}_i^{(t+1)})$ and lines 22 and 23 are removed, the original improved MO-CMA-ES is obtained.

7 EXPERIMENT ON MULTI-OBJECTIVE OPTIMIZATION PROBLEMS: HYPERPARAMETER SENSITIVITY FOR α

In this section, we apply MO-CMA-ES with Margin to several multi-objective MI-BBO benchmark functions and validate its robustness and efficiency as same as Section 5.

As a benchmark function involving continuous and binary variables, we consider DSLOTZ, which combines DOUBLESPHERE and LEADINGONESTAILINGZEROS (LOTZ). The DOUBLESPHERE function is a benchmark function to minimize two SPHERE functions $f_1(x) = \sum_{i=1}^N x_i^2$ and $f_2(x) = \sum_{i=1}^N (1 - x_i)^2$. The Pareto set of DOUBLESPHERE can be expressed analytically; the line segment between the point minimizes f_1 and f_2 . The LOTZ function is a benchmark function to maximize two functions $f_1(x) = \sum_{i=1}^N \prod_{j=1}^i x_j$ and $f_2(x) = \sum_{i=1}^N \prod_{j=i}^n (1 - x_j)$. The first objective f_1 is the LEADINGONES

Algorithm 3: Single update in MO-CMA-ES with Margin

```

1: given  $Q^{(t)}$ 
2: for  $i = 1, \dots, \lambda$  do
3:    $\mathbf{a}'_i^{(t+1)} \leftarrow \mathbf{a}_i^{(t)}$ 
4:    $\mathbf{y}_i \sim \mathcal{N}(\mathbf{0}, \mathbf{C}_i^{(t)})$ 
5:    $\mathbf{x}'_i^{(t+1)} \leftarrow \mathbf{x}_i^{(t)} + \sigma_i^{(t)} \mathbf{y}_i$ 

6:    $\mathbf{v}'_i^{(t+1)} \leftarrow \mathbf{x}_i^{(t)} + \sigma_i^{(t)} \mathbf{A}_i^{(t)} \mathbf{y}_i^\top$ 
7:    $\bar{\mathbf{v}}'_i^{(t+1)} \leftarrow \text{ENCODING}_f(\mathbf{v}'_i^{(t+1)})$ 

8:    $Q^{(t)} \leftarrow Q^{(t)} \cup \{\mathbf{a}'_i^{(t+1)}\}$ 
9: end for
10: for  $i = 1, \dots, \lambda$  do
11:    $\bar{p}'_{\text{succ},i}^{(t+1)} \leftarrow (1 - c_p) \bar{p}'_{\text{succ},i}^{(t+1)} + c_p \text{succ}_{Q^{(t)}}(\mathbf{a}_i^{(t)}, \mathbf{a}'_i^{(t+1)})$ 
12:    $\sigma'_i^{(t+1)} \leftarrow \sigma'_i^{(t+1)} \exp\left(\frac{1}{d} \frac{\bar{p}'_{\text{succ},i}^{(t+1)} - p_{\text{succ}}^{\text{target}}}{1 - p_{\text{succ}}^{\text{target}}}\right)$ 
13:   if  $\bar{p}'_{\text{succ},i}^{(t+1)} < p_{\text{thresh}}$  then
14:      $\mathbf{p}'_{c,i}^{(t+1)} \leftarrow (1 - c_c) \mathbf{p}'_{c,i}^{(t+1)} + \sqrt{c_c(2 - c_c)} \frac{\mathbf{x}'_i^{(t+1)} - \mathbf{x}_i^{(t)}}{\sigma_i^{(t)}}$ 
15:      $\mathbf{C}'_i^{(t+1)} \leftarrow (1 - c_{\text{cov}}) \mathbf{C}'_i^{(t+1)} + c_{\text{cov}} \mathbf{p}'_{c,i}^{(t+1)} \mathbf{p}'_{c,i}^{(t+1)^\top}$ 
16:   else
17:      $\mathbf{p}'_{c,i}^{(t+1)} \leftarrow (1 - c_c) \mathbf{p}'_{c,i}^{(t+1)}$ 
18:      $\mathbf{C}'_i^{(t+1)} \leftarrow (1 - c_{\text{cov}}) \mathbf{C}'_i^{(t+1)} + c_{\text{cov}} \left( \mathbf{p}'_{c,i}^{(t+1)} \mathbf{p}'_{c,i}^{(t+1)^\top} + c_c(2 - c_c) \mathbf{C}'_i^{(t+1)} \right)$ 
19:   end if
20:    $\bar{p}_{\text{succ},i}^{(t)} \leftarrow (1 - c_p) \bar{p}_{\text{succ},i}^{(t)} + c_p \text{succ}_{Q^{(t)}}(\mathbf{a}_i^{(t)}, \mathbf{a}'_i^{(t+1)})$ 
21:    $\sigma_i^{(t)} \leftarrow \sigma_i^{(t)} \exp\left(\frac{1}{d} \frac{\bar{p}_{\text{succ},i}^{(t)} - p_{\text{succ}}^{\text{target}}}{1 - p_{\text{succ}}^{\text{target}}}\right)$ 

22:    $\mathbf{x}'_i^{(t+1)}, \mathbf{A}'_i^{(t+1)} \leftarrow \text{MarginCorrection}\left(\mathbf{x}'_i^{(t+1)}, \mathbf{A}'_i^{(t+1)}, \sigma'_i^{(t+1)}, \mathbf{C}'_i^{(t+1)}\right)$ 
23:    $\mathbf{x}_i^{(t)}, \mathbf{A}_i^{(t)} \leftarrow \text{MarginCorrection}\left(\mathbf{x}_i^{(t)}, \mathbf{A}_i^{(t)}, \sigma_i^{(t)}, \mathbf{C}'_i^{(t)}\right)$ 

24: end for
25:  $Q^{(t+1)} \leftarrow \left\{ Q_{<:i}^{(t)} \mid 1 \leq i \leq \lambda \right\}$ 

```

function, which counts the number of leading ones of the bit string. On the other hand, the second objective f_2 counts the number of tailing zeros. The Pareto set of LOTZ consists of $1^N, 1^{N-1}0, \dots, 10^{N-1}, 0^N$.

Additionally, as a benchmark function involving continuous and integer variables, we consider DSINT, in which some variables of DOUBLESPHERE are integerized. However, when the DOUBLESPHERE function that minimizes $f_1(x) = \sum_{i=1}^N x_i^2$ and $f_2(x) = \sum_{i=1}^N (1 - x_i)^2$ partially is integerized, the integer variable part of the Pareto set can only take $0^{N_{\text{in}}}$ or $1^{N_{\text{in}}}$, making the optimization of the integer variable part too easy. Therefore, we verify the DOUBLESPHERE that minimizes $f_1(x) = \sum_{i=1}^N x_i^2$ and $f_2(x) = \sum_{i=1}^N (10 - x_i)^2$ with a partially discretized function.

The definitions of the benchmark functions in this section are listed as below:

- DSLOTZ (DOUBLESPHERELEADINGONESTAILINGZEROS)

$$f_1(\bar{x}) = \frac{1}{N_{\text{co}}} \left(\sum_{j=1}^{N_{\text{co}}} [\bar{x}]_j^2 \right) + \frac{1}{N_{\text{bi}}} \left(N_{\text{bi}} - \sum_{k=N_{\text{co}}+1}^N \prod_{l=N_{\text{co}}+1}^k [\bar{x}]_l \right) \quad (49)$$

$$f_2(\bar{x}) = \frac{1}{N_{\text{co}}} \left(\sum_{j=1}^{N_{\text{co}}} (1 - [\bar{x}]_j)^2 \right) + \frac{1}{N_{\text{bi}}} \left(N_{\text{bi}} - \sum_{k=N_{\text{co}}+1}^N \prod_{l=k}^N (1 - [\bar{x}]_l) \right) \quad (50)$$

- DSINT (DOUBLESPHEREINT)

$$f_1(\bar{x}) = \frac{1}{N_{\text{co}}} \left(\frac{1}{10^2} \sum_{j=1}^{N_{\text{co}}} [\bar{x}]_j^2 \right) + \frac{1}{N_{\text{in}}} \left(\frac{1}{10^2} \sum_{k=N_{\text{co}}+1}^N [\bar{x}]_k^2 \right) \quad (51)$$

$$f_2(\bar{x}) = \frac{1}{N_{\text{co}}} \left(\frac{1}{10^2} \sum_{j=1}^{N_{\text{co}}} (10 - [\bar{x}]_j)^2 \right) + \frac{1}{N_{\text{in}}} \left(\frac{1}{10^2} \sum_{k=N_{\text{co}}+1}^N (10 - [\bar{x}]_k)^2 \right) \quad (52)$$

In all functions, the first N_{co} variables are continuous wheres the last $N - N_{\text{co}}$ variables are binary or integer. In all experiments, we adopt the default parameters of improved MO-CMA-ES as given in [Voß et al. 2010], and set a reference point as $[5, 5]$.

The step-size and covariance matrix are initialized as $\sigma_i^{(0)} = 1$, $C_i^{(0)} = \mathbf{I}$ for the DSLOTZ function and $\sigma_i^{(0)} = 5$, $C_i^{(0)} = \mathbf{I}$ for the DSINT function. The initial search point $\bar{x}_i^{(0)}$ is set to uniform random values in the range $[0, 1]$ for continuous and binary variables. The optimization is stopped when the iteration t is reached $10^4 N$. As with Section 5.1, the hyperparameter α should depend on the number of dimensions N and sample size λ . Unfortunately, unlike the original CMA-ES, MO-CMA-ES does not have a recommended value for the sample size. Therefore, we use three different sample sizes $\lambda \in \{10, 50, 100\}$. The number of dimensions of N is set to 10, 20 or 30, and $N_{\text{co}} = N_{\text{bi}} = N/2$. In this experiment, we evaluate hypervolume after optimization of $\alpha = N^{-m} \lambda^{-m}$ ($m, n \in \{0, 0.5, 1, 1.5, 2, 2.5, 3\}$) except $\alpha = 1$. In each setting, 100 trials are performed independently using different seed values.

Results and Discussion. Figure 4 shows the difference in median hypervolume for DSLOTZ function after optimization between MO-CMA-ES with Margin and MO-CMA-ES without margin for each setting.

For $\mu = \lambda = 10$ (top in Figure 4) and $N = 10$, there is no significant difference between the median hypervolumes of MO-CMA-ES and MO-CMA-ES with Margin, but MO-CMA-ES with Margin has the worst performance when $\alpha = N^{-0.5}, \lambda^{-0.5}$. For $\mu = \lambda = 10$ and $N = 20, 30$, MO-CMA-ES with Margin had worse median hypervolume than MO-CMA-ES when $\alpha = \lambda^{-0.5}$, but other settings improved it by 0.1–0.3 for $N = 20$ and by more than 1 for $N = 30$.

For $\mu = \lambda = 50, 100$ (middle and bottom in Figure 4) and $N = 10$, there is no significant difference between the median hypervolumes of MO-CMA-ES and MO-CMA-ES with Margin as same as the case of $\mu = \lambda = 10$. For $\mu = \lambda = 50, 100$ and $N = 20, 30$, MO-CMA-ES with Margin for $\alpha = N^{-0.5}, \lambda^{-0.5}$ except for $N = 20$ has a worse median hypervolume than MO-CMA-ES, but in other settings, MO-CMA-ES with Margin performs competitively with MO-CMA-ES.

Next, Figure 5 shows the difference in median hypervolume for DSINT function after optimization between MO-CMA-ES with Margin and MO-CMA-ES without margin for each setting. The DSINT function also shows that MO-CMA-ES with Margin for $\alpha = \lambda^{-0.5}, N^{-0.5}$ has the worst hypervolume after optimization, but other settings, MO-CMA-ES with Margin performs competitively with MO-CMA-ES.

In summary, MO-CMA-ES with Margin except in the case of $\alpha = \lambda^{-0.5}, N^{-0.5}$ can obtain the well or higher hypervolume than MO-CMA-ES. In particular, the smaller the sample size and the higher the dimension settings, the

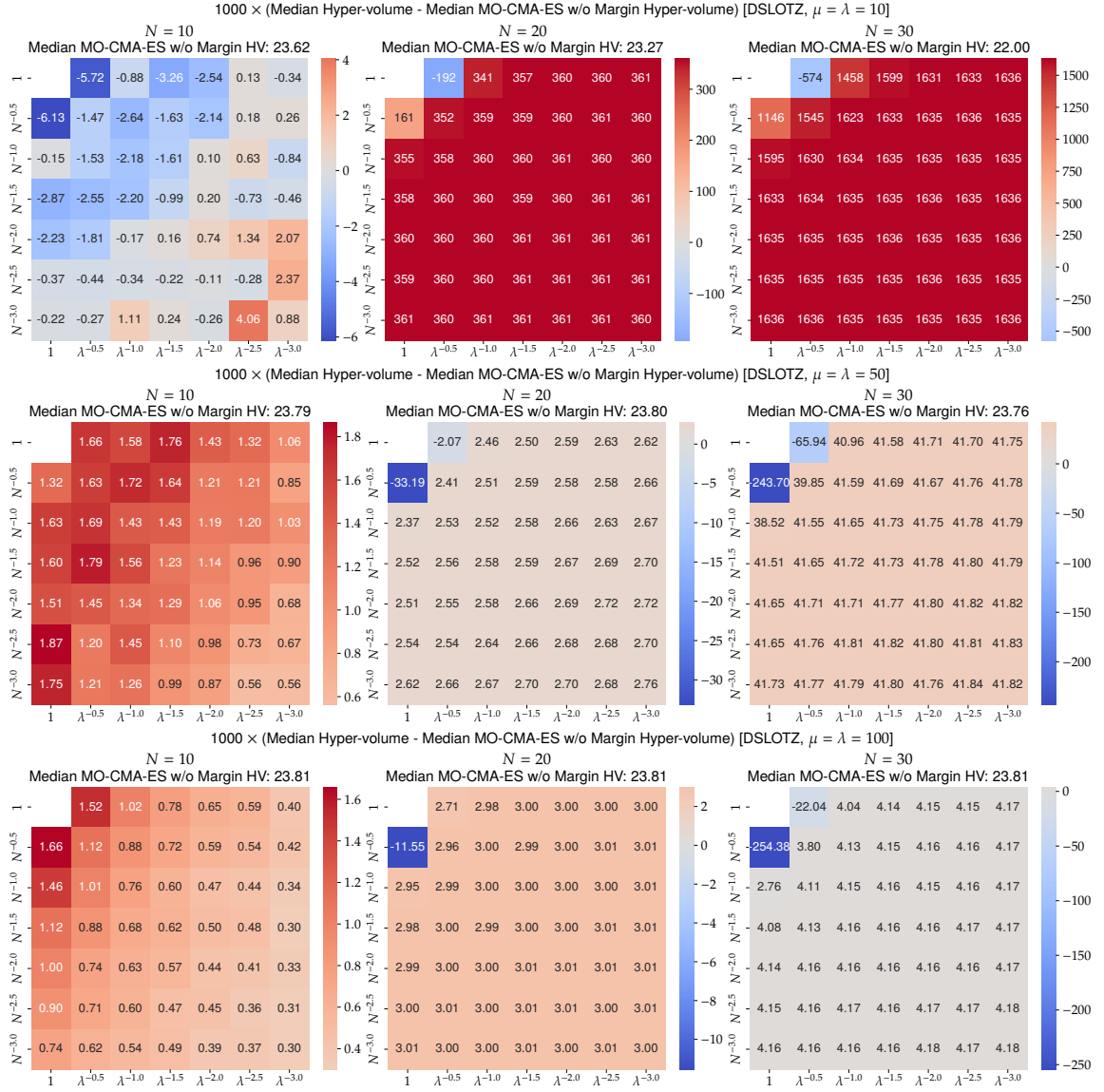


Fig. 4. Heatmap of difference in median hypervolume after optimization between MO-CMA-ES with Margin and MO-CMA-ES without margin in the N -dimensional DSLOTZ function with $\mu = \lambda = 10$ (top), 50 (middle), 100 (bottom) when the hyperparameter $\alpha = N^{-m} \lambda^{-n}$ of the MO-CMA-ES with Margin is changed.

better the effect of the margin. As with the single objective, a large value such as $\alpha = N^{-0.5}, \lambda^{-0.5}$ is considered to have worsened the hypervolume compared to MO-CMA-ES because the search is unstable. On the other hand, for the other settings, there is no significant difference in the results of MO-CMA-ES with Margin.

Therefore, we compare the speed of improvement of the hypervolumes for different α settings to determine a recommended value for α . Figure 6 shows the comparison of the transition of median hypervolumes of the first 1000

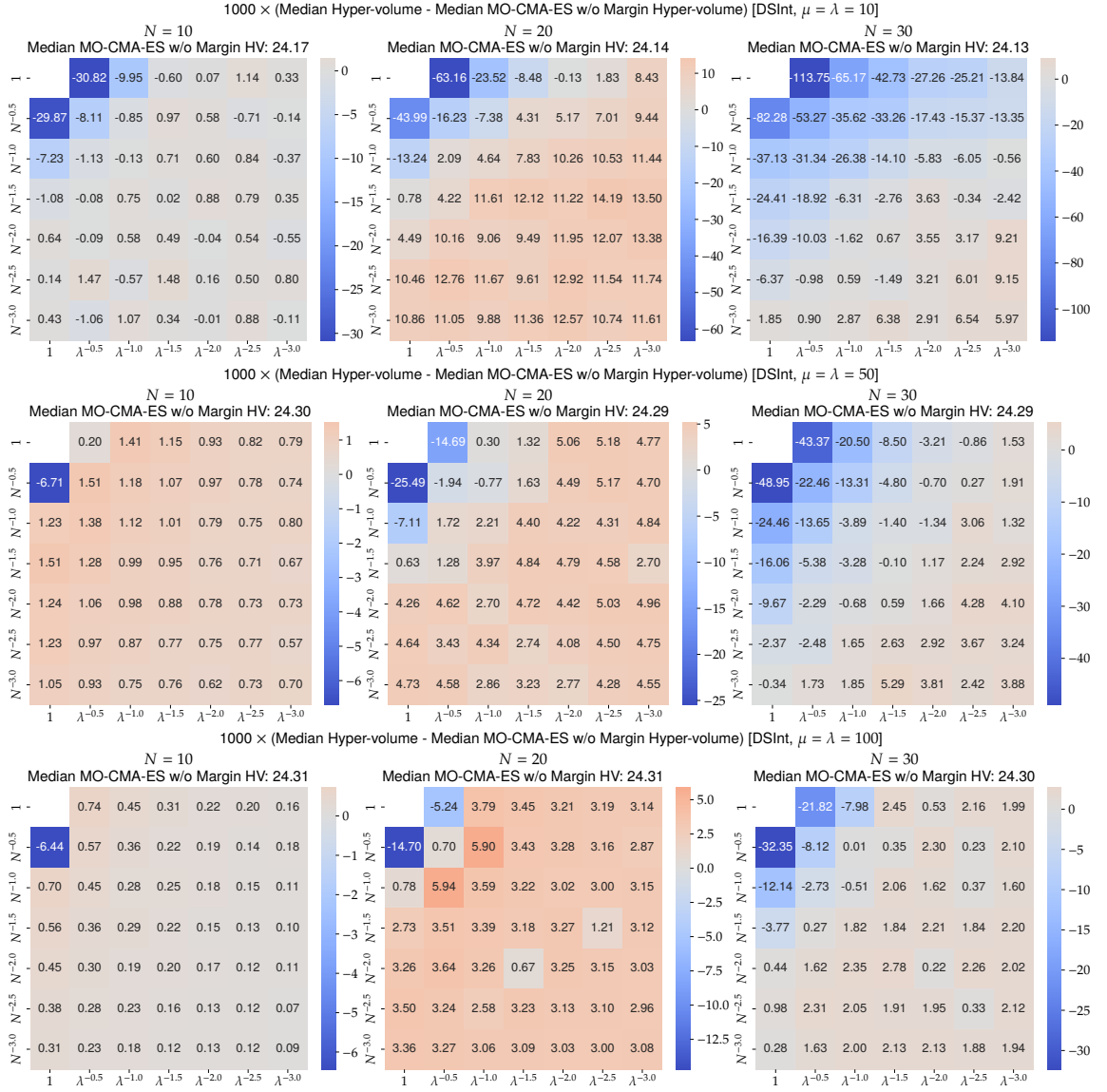


Fig. 5. Heatmap of difference in median hypervolume after optimization between MO-CMA-ES with Margin and MO-CMA-ES without margin in the N -dimensional DSInt function with $\mu = \lambda = 10$ (top), 50 (middle), 100 (bottom) when the hyperparameter $\alpha = N^{-m} \lambda^{-n}$ of the MO-CMA-ES with Margin is changed.

iterations on DSINT and DSLOTZ functions of $N = 30$ for MO-CMA-ES with Margin at $\alpha = (N\lambda)^{-3}, (N\lambda)^{-2}, (N\lambda)^{-1}$ and MO-CMA-ES on $\mu = \lambda = 10$. The DSINT function shows no significant difference in hypervolume transition for different values of α . The reason for this is the ease of obtaining a Pareto set of the DSINT function. In single-objective SPHEREINT function optimization, if the integer variable in any one dimension was fixed at a non-optimal integer, it was difficult to obtain an optimal solution. In the DSINT function, on the other hand, even if an integer variable in one

dimension is fixed, one of the Pareto-optimal solutions can be obtained by optimizing the other integer variables. In addition, another reason that facilitates the optimization of the DSINT function is that even if some of the λ individuals become fixed in a completely inferior solution, it can be solved by mutations from other individuals.

On the other hand, in the Dslotz function, the difference in hypervolume transition is observed after the 400 iterations. The MO-CMA-ES without Margin shows optimization has almost stalled. This is because the optimization of the binary variables is not working well due to fixation. In fact, we found by experiments that the obtained solution set contained solutions with binary variable parts other than $1^{N_{bi}}, 1^{N_{bi}-1}, \dots, 10^{N_{bi}-1}, 0^{N_{bi}}$. For $\alpha = (N\lambda)^{-3}$, the hypervolume increases slowly, but after 1000 iterations, it reaches about the same hypervolume as the other α settings. For $\alpha = (N\lambda)^{-2}, (N\lambda)^{-1}$, hypervolumes of both settings increase at about the same rate, but $\alpha = (N\lambda)^{-1}$ shows a smoother increasing in hypervolume.

Based on these results, we recommend $\alpha = (N\lambda)^{-1}$ for MO-CMA-ES with Margin due to its robustness and efficiency. This recommendation can be shared with single-objective case and will be enjoyed by users because it reduces the need for tedious parameter tuning.

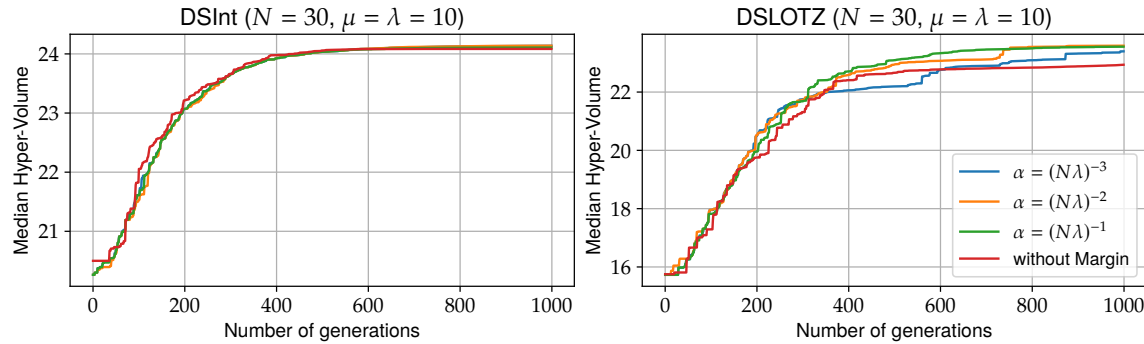


Fig. 6. Transition of median hypervolumes of the first 1000 iterations on DSInt (left) and Dslotz (right) functions for MO-CMA-ES with and without Margin.

8 CONCLUSION

In this work, we first experimentally confirmed that the existing integer handling method, CMA-ES-IM [Hansen 2011] with or without the box constraint, does not work effectively for binary variables, and then proposed a new integer variable handling method for CMA-ES. In the proposed method, the mean vector and the diagonal affine transformation matrix for the covariance matrix are corrected so that the marginal probability for an integer variable is lower-bounded at a certain level, which is why the proposed method is called the CMA-ES with *margin*; it considers both the binary and integer variables. To demonstrate the generality of the idea of the proposed method, in addition to the single-objective optimization case, we also develop multi-objective CMA-ES with Margin (MO-CMA-ES with Margin), which is aimed at multi-objective mixed-integer optimization. We confirmed by experiment the behavior of the MO-CMA-ES with Margin on DOUBLESPHERELOTZ and DOUBLESPHEREINT, which we used as bi-objective mixed-integer benchmark problems.

The proposed method has a hyperparameter, α , that determines the degree of the lower bound for the marginal probability. We investigated the change in the optimization performance with multiple α settings in order to determine the default parameter. With the recommended value of α , we experimented the proposed method on several (MO)-MIBBO benchmark problems. The experimental results demonstrated that in the single-objective optimization case, the

proposed method is robust even when the number of dimensions increases and can find the optimal solution with fewer evaluations than the existing method, CMA-ES-IM with or without the box constraint. In the multi-objective optimization case, compared to MO-CMA-ES, MO-CMA-ES with Margin achieved better or at least competitive performance in the experiments with most of α settings. The effect of the margin was clear especially with the small sample size and/or the high-dimensional settings.

There are still many challenges left for the MI-BBO; for example, Tušar et al. [2019] pointed out the difficulty of optimization for non-separable ill-conditioned convex-quadratic functions, such as the rotated Ellipsoid function. In the future, we need to address these issues, which have not yet been addressed by the proposed or existing methods, by considering multiple dimension correlations. Additionally, evaluating the proposed method on real-world MI-BBO problems, including multi-objective optimization, is also an important future direction.

ACKNOWLEDGMENTS

This work was partially supported by JSPS KAKENHI Grant Number JP20H04240 and JST PRESTO Grant Number JPMJPR2133. A portion of this paper was based on the results obtained from the project JPNP18002 commissioned by the New Energy and Industrial Technology Development Organization (NEDO).

REFERENCES

Youhei Akimoto, Shinichi Shirakawa, Nozomu Yoshinari, Kento Uchida, Shota Saito, and Kouhei Nishida. 2019. Adaptive Stochastic Natural Gradient Method for One-Shot Neural Architecture Search. In *Proceedings of the 36th International Conference on Machine Learning (ICML)*, Vol. 97. 171–180.

Shummet Baluja. 1994. *Population-Based Incremental Learning: A Method for Integrating Genetic Search Based Function Optimization and Competitive Learning*. Technical Report CMU-CS-94-163. Carnegie Mellon University.

Laurens Bliek, Arthur Guijt, Sicco Verwer, and Mathijs de Weerdt. 2021. Black-Box Mixed-Variable Optimisation Using a Surrogate Model That Satisfies Integer Constraints. In *Proceedings of the Genetic and Evolutionary Computation Conference Companion* (Lille, France). ACM, New York, NY, USA, 1851–1859. <https://doi.org/10.1145/3449726.3463136>

K. Deb, A. Pratap, S. Agarwal, and T. Meyarivan. 2002. A fast and elitist multiobjective genetic algorithm: NSGA-II. *IEEE Transactions on Evolutionary Computation* 6, 2 (2002), 182–197. <https://doi.org/10.1109/4235.996017>

Michael Emmerich, Nicola Beume, and Boris Naujoks. 2005. An EMO Algorithm Using the Hypervolume Measure as Selection Criterion. In *Evolutionary Multi-Criterion Optimization*, Carlos A. Coello Coello, Arturo Hernández Aguirre, and Eckart Zitzler (Eds.). Springer Berlin Heidelberg, Berlin, Heidelberg, 62–76.

Garuda Fujii, Masayuki Takahashi, and Youhei Akimoto. 2018. CMA-ES-based structural topology optimization using a level set boundary expression—Application to optical and carpet cloaks. *Computer Methods in Applied Mechanics and Engineering* 332 (April 2018), 624–643. <https://doi.org/10.1016/j.cma.2018.01.008>

Ryoki Hamano, Shota Saito, Masahiro Nomura, and Shinichi Shirakawa. 2022. CMA-ES with Margin: Lower-Bounding Marginal Probability for Mixed-Integer Black-Box Optimization. In *Proceedings of the Genetic and Evolutionary Computation Conference* (Boston, Massachusetts) (GECCO '22). Association for Computing Machinery, New York, NY, USA, 639–647. <https://doi.org/10.1145/3512290.3528827>

Nikolaus Hansen. 2011. *A CMA-ES for Mixed-Integer Nonlinear Optimization*. Research Report. INRIA.

Nikolaus Hansen. 2016. The CMA evolution strategy: A tutorial. *arXiv preprint arXiv:1604.00772* (2016).

Nikolaus Hansen, Sibylle D. Müller, and Petros Koumoutsakos. 2003. Reducing the Time Complexity of the Derandomized Evolution Strategy with Covariance Matrix Adaptation (CMA-ES). *Evolutionary Computation* 11, 1 (March 2003), 1–18. <https://doi.org/10.1162/106365603321828970>

N. Hansen and A. Ostermeier. 1996. Adapting arbitrary normal mutation distributions in evolution strategies: the covariance matrix adaptation. In *Proceedings of IEEE International Conference on Evolutionary Computation*. 312–317. <https://doi.org/10.1109/ICEC.1996.542381>

Elad Hazan, Adam Klivans, and Yang Yuan. 2018. Hyperparameter optimization: a spectral approach. In *International Conference on Learning Representations (ICLR)*.

Frank Hutter, Lars Kotthoff, and Joaquin Vanschoren. 2019. *Automated Machine Learning : Methods, Systems, Challenges*. Springer, Cham. <https://doi.org/10.1007/978-3-030-05318-5>

Christian Igel, Nikolaus Hansen, and Stefan Roth. 2007. Covariance matrix adaptation for multi-objective optimization. *Evolutionary computation* 15, 1 (2007), 1–28.

Akshay Iyer, Yichi Zhang, Aditya Prasad, Praveen Gupta, Siyu Tao, Yixing Wang, Prajakta Prabhune, Linda S. Schadler, L. Catherine Brinson, and Wei Chen. 2020. Data centric nanocomposites design via mixed-variable Bayesian optimization. *Molecular Systems Design & Engineering* 5, 8 (Sept. 2020), 1376–1390. <https://doi.org/10.1039/DOME00079E>

Rui Li, Michael T.M. Emmerich, Jeroen Eggermont, Thomas Bäck, M. Schütz, J. Dijkstra, and J.H.C. Reiber. 2013. Mixed Integer Evolution Strategies for Parameter Optimization. *Evolutionary Computation* 21, 1 (March 2013), 29–64. https://doi.org/10.1162/EVCO_a_00059

Atsuhiko Miyagi, Youhei Akimoto, and Hajime Yamamoto. 2018. Well Placement Optimization for Carbon Dioxide Capture and Storage via CMA-ES with Mixed Integer Support. In *Proceedings of the Genetic and Evolutionary Computation Conference Companion* (Kyoto, Japan) (GECCO '18). ACM, New York, NY, USA, 1696–1703. <https://doi.org/10.1145/3205651.3205706>

S. Tamilselvi and S. Baskar. 2014. Modified parameter optimization of distribution transformer design using covariance matrix adaptation evolution strategy. *International Journal of Electrical Power & Energy Systems* 61 (2014), 208–218. <https://doi.org/10.1016/j.ijepes.2014.03.039>

Tea Tušar, Dimo Brockhoff, and Nikolaus Hansen. 2019. Mixed-integer benchmark problems for single- and bi-objective optimization. In *Proceedings of the Genetic and Evolutionary Computation Conference* (Prague, Czech Republic). ACM, New York, NY, USA, 718–726. <https://doi.org/10.1145/3321707.3321868>

Thomas Voß, Nikolaus Hansen, and Christian Igel. 2010. Improved step size adaptation for the MO-CMA-ES. In *Proceedings of the 12th annual conference on Genetic and evolutionary computation*, 487–494.

Jinn-Moon Yang and Cheng-Yan Kao. 1998. An evolutionary algorithm for synthesizing optical thin-film designs. In *Proceedings of Parallel Problem Solving from Nature (PPSN) V*. Springer, Berlin, Heidelberg, 947–956. <https://doi.org/10.1007/BFb0056936>

Yichi Zhang, Daniel W. Apley, and Wei Chen. 2020. Bayesian Optimization for Materials Design with Mixed Quantitative and Qualitative Variables. *Scientific Reports* 10, 1 (March 2020), 4924. <https://doi.org/10.1038/s41598-020-60652-9>

Eckart Zitzler and Lothar Thiele. 1998. Multiobjective optimization using evolutionary algorithms — A comparative case study. In *Parallel Problem Solving from Nature — PPSN V*, Agoston E. Eiben, Thomas Bäck, Marc Schoenauer, and Hans-Paul Schwefel (Eds.). Springer Berlin Heidelberg, Berlin, Heidelberg, 292–301.